



State-of-the-art overview of pipeline steel corrosion in impure dense CO₂ for CCS transportation: mechanisms and models

Yong Xiang, Minghe Xu & Yoon-Seok Choi

To cite this article: Yong Xiang, Minghe Xu & Yoon-Seok Choi (2017) State-of-the-art overview of pipeline steel corrosion in impure dense CO₂ for CCS transportation: mechanisms and models, Corrosion Engineering, Science and Technology, 52:7, 485-509, DOI: [10.1080/1478422X.2017.1304690](https://doi.org/10.1080/1478422X.2017.1304690)

To link to this article: <http://dx.doi.org/10.1080/1478422X.2017.1304690>



Published online: 28 Mar 2017.



Submit your article to this journal [↗](#)



Article views: 83



View related articles [↗](#)



View Crossmark data [↗](#)



Citing articles: 1 View citing articles [↗](#)



State-of-the-art overview of pipeline steel corrosion in impure dense CO₂ for CCS transportation: mechanisms and models

Yong Xiang^{a,b}, Minghe Xu^c and Yoon-Seok Choi^d

^aCollege of Mechanical and Transportation Engineering, China University of Petroleum, Beijing, PR China; ^bBeijing Key Laboratory of Process Fluid Filtration and Separation, China University of Petroleum, Beijing, PR China; ^cDepartment of Thermal Engineering, State Key Laboratory of Power Systems, Tsinghua University, Beijing, PR China; ^dDepartment of Chemical and Biomolecular Engineering, Institute for Corrosion and Multiphase Technology, Ohio University, Athens, OH, USA

ABSTRACT

This work reviews the existing open literature concerned with pipeline steel corrosion in CO₂-rich phase with impurities for carbon capture and storage purpose. The intent of this review was to provide information on the corrosion mechanisms, which is crucial for establishing the mechanistic prediction models. The primary focus was placed on key affecting parameters and their corresponding mechanisms, while the corrosion control strategies and research prospects are also discussed. This review covers the effects of: impurities, pressure, temperature, flow, exposure time, product layers, and steel chemistry. The influences of flow dynamics, amines, sulphur, and solids that had received little systematic attention need to be further addressed. Contradictory conclusions regarding the influence of H₂O and O₂ on the corrosion rates should be re-evaluated. The localised corrosion and cathodic reaction mechanisms also require further investigation, especially under synergistic conditions with multiple impurities.

ARTICLE HISTORY

Received 13 December 2016
Accepted 5 March 2017

KEYWORDS

CCS; impure dense CO₂; corrosion mechanism; prediction model; synergistic effect; localised corrosion

Nomenclature

A_ϕ	Debye–Hückel equation constant
b_1	modified TCPC model parameter
c_j	mole concentration for species j , mol L ⁻¹
CR	corrosion rate, mm a ⁻¹
d_f	product film thickness, m
D_j	diffusion coefficient for species j , m ² s ⁻¹
EW	equivalent mass, kg
i_{H^+}	hydrogen electrode current density, A m ⁻²
i_{O_2}	oxygen electrode current density, A m ⁻²
i_{Fe}	anode current density, A m ⁻²
I	ionic strength, mol kg ⁻¹
k_G	effective crystal growth rate constant
K_c	corrosion rate equation coefficient
K_{IC}	fracture toughness of product scale, MPa m ^{1/2}
n_1	modified TCPC model parameter
R_j	chemical reaction rate for species j , mol m ⁻³ s ⁻¹
R_G	precipitation rate, kg m ⁻² s ⁻¹
S_1	modified TCPC model parameter
t	time, s
T	temperature, K
ϵ	volumetric porosity of product scale
v_+	chemical equivalent coefficient of cation
v_-	chemical equivalent coefficient of anion
x	x coordinate
z	component charge number
ρ	density, kg m ⁻³
Δc	mass concentration difference, kg kg ⁻¹
γ	activity coefficient

Introduction

Pipeline transportation is one of the main ways to transport CO₂ to sequestration sites, either in the oil and gas industry for the purpose of enhanced oil recovery (EOR) or in carbon capture and storage (CCS) systems for the purpose of greenhouse gas control. CO₂ transportation by pipeline has been in

progress for more than 40 years, and over 6000 km of CO₂ pipelines currently exist for EOR, mainly situated in the U.S.A and Canada. The existing CO₂ transportation systems, which are summarised in Table 1, always require high-purity CO₂ streams, especially for EOR, which transports CO₂ from natural sources [1]. However, for future anthropogenic CO₂ transportation in the CCS industry, the CO₂ stream will further contain a certain amount of flue gas impurities (SO_x, NO_x, HCl, CO, O₂, Ar, and H₂), in addition to H₂S, CH₄, N₂, and H₂O, depending on fuel sources, combustion methods and CO₂ capture technologies. Unfortunately, purifying the CO₂ stream to relatively high purity will be costly, which will not be an option in future large-scale CCS system. Although the co-sequestration of CO₂ and impurities may greatly reduce the cost of the purification process, further evidence is needed to show whether it is safe for long-distance transportation and permanent geological sequestration. The CO₂ commercial projects under construction or planning are summarised in Table 2, and all the CO₂ involved is from anthropogenic sources.

Usually, the pipeline steel type for CO₂ transportation is carbon steel, such as X52, X65, and X70. These CO₂ pipeline steels may suffer severe corrosion degradation problems due to the attack by impurities, thus deteriorating the operational integrity of CO₂ pipeline transportation systems. According to a report by Det Norske Veritas (DNV) based on the data provided by the Pipeline and Hazardous Materials Safety Administration (PHMSA) of the US Department of Transportation, 29 incidents with regard to CO₂ transmission were reported from 1986 to 2008, and 45% of these incidents were caused by corrosion, ranking first among all causes [2]. Corrosion is also a common concern in all CCS processes, including capture, transportation, and injection [3–9]. Unlike

Table 1. Summary of the existing long-distance CO₂ pipelines [59,60].

Project name	Operator	Country	Capacity (Mt a ⁻¹)	Length (km)	Diameter (mm)	Pressure (MPa)	Completion time	CO ₂ source
NEJD	Denbury Resources	U.S.A	–	295	508	–	1976	Jackson Dome
Cortez	Kinder Morgan	U.S.A	19.3	808	762	18.6	1984	McElmo Dome
Sheep Mountain	BP	U.S.A	6.3/9.2	296/360	508/610	13.2	1983	Sheep Mountain
Bravo	BP	U.S.A	7.3	350	508	16.5	1984	Bravo Dome
Transpetco Bravo	Transpetco	U.S.A	3.3	193	324	–	–	–
Central Basin	Kinder Morgan	U.S.A	11.5	278	508/660/610/ 508/406	15.1/15.1/15.8/ 16.5/17.2	–	–
Este	Exxon Mobil	U.S.A	4.8	191	305/356	–	–	–
West Texas	Trinity	U.S.A	1.9	204	203–305	–	–	–
SACROC	–	U.S.A	4.2	354	406	17.5	1972	Gasification
Val Verde	–	U.S.A	2.5	130	–	–	1998	Val Verde Gas Plants
Canyon Reef Carriers	Kinder Morgan	U.S.A	4.6	225	406	–	–	–
Bati Raman	Turkish Petroleum	Turkey	1.1	90	–	17.0	1983	Dodan field
Weyburn	Dakota Gasification Company	U.S.A and Canada	4.6	330	305–356	20.4	2000	Gasification
Snøhvit	StatoilHydro	Norway	0.7	153	203	15	2007	LNG plant

Table 2. Summary of CO₂ commercial projects under construction or planning [61].

Country	Project	Operator	Fuel	Scale/MW	Capture technology	CO ₂ purpose	Status
U.S.A	Kemper County	Southern	Coal	582	Pre	EOR	Under construction
	Petra Nova WA Parish	NRG Energy JX Nippon	Coal	240	Post	EOR	Under construction
	HECA	SCS	Petcoke	405	Pre	EOR	Planning
	TCEP	Summit Power	Coal	400	Pre	EOR	Planning
Canada	Bow City	BCPL	Coal	1000	Post	EOR	Planning
Norway	Longyearbyen	Unis CO ₂	Coal	N/A	Post	Saline	Planning
Korea	Korea CCS	KCRC	Coal	500	Oxy	Saline	Planning
European Union	ROAD	E.ON	Coal	250	Post	Depleted oil or gas	Planning
	Magnum	Nuon	Various	1200	Pre	Depleted oil or gas	Planning
	Peterhead	Shell and SSE	Gas	385	Post	Depleted gas	Planning
	Captain	Summit Power	Coal	570	Post	Saline	Planning
	White Rose	Capture Power	Coal	426	Oxy	Saline	Planning
	Killingholme	C.GEN	Coal	470	Pre	Saline	Planning
	Daqing	Alstom & Datang	Coal	350	Oxy	EOR	Planning
China	Dongguan	Dongguan Taiyangzhou Power Corporation	Coal	800	Pre	EOR	Planning
	Shengli Oil Field	Sinopec	Coal	250	Post	EOR	Planning
	GreenGen	GreenGen	Coal	400	Pre	EOR	Planning
	Lianyungang	Lianyungang Clean Energy	Coal	1200	Pre	Saline or EOR	Planning

the corrosion of steels under low CO₂ partial pressure conditions, which has been widely addressed in the oil and gas industry, the steel corrosion issue under high partial CO₂ pressure during the CCS transportation process, either in the supercritical phase or the liquid CO₂ phase (both can be called dense CO₂ or a CO₂-rich phase), still lacks adequate related research.

Research on the corrosion of carbon steel in dense CO₂ was initiated in 1975, aiming at the material selection of CO₂ pipeline transportation for EOR. This study showed no localised corrosion on X60 steel and fairly low general corrosion rates [10]. The US Department of Energy also performed some research related to supercritical CO₂ corrosion in 1979 [11] and 1996 [12], which also indicated a low corrosion rate of steel when the water concentration was low. Currently, studies on steel corrosion in dense phase CO₂ with impurities for CCS have mainly focused on influential parameters, corrosion product layers (structure, morphology, composition) [13–15], corrosion mechanisms [16–18], and mathematical prediction models [19–21]. The studies on influential parameters are crucial, since they provide basic information to uncover the correlations between corrosion phenomena and mechanisms, based on which the corrosion prediction models, corrosion control strategies and pipeline integrity management can be further manipulated.

The internal corrosion of pipeline steel in dense CO₂ with impurities is influenced by a variety of parameters, including environmental, metallurgical, and physical variables. A number of these influential parameters have been preliminarily investigated, such as the impurities (moisture, acidic gases, O₂, and the other impurities), partial pressure, temperature, flow, exposure time, product scales, and materials [13,15,16,19,21–52]. These parameters not only affect the extent of corrosion independently but also accelerate or mitigate macroscopic corrosion through cross-reactions and interactions between them, thus generating synergistic or competitive effects. Systematically checking whether all the important influential parameters have been addressed in the open literature and the research progress in relation to dense CO₂ corrosion is essential for further understanding of the corrosion mechanisms of steel in a dense CO₂ environment, as well as for establishing mechanistic prediction models.

Therefore, this work reviews the existing research development in the open literature and focuses on the influential mechanisms of various parameters on pipeline steel corrosion in dense CO₂ with impurities. The influential parameters neglected by the current research are also mentioned and analysed. The existing mathematical prediction models for dense CO₂ corrosion prediction are highlighted. Moreover, the knowledge gaps and areas requiring further research are proposed in this work.

Generally, two types of dense CO₂ corrosion problems can occur: corrosion in a water-saturated dense CO₂ phase and corrosion in a dense CO₂-saturated water phase. The former scenario is usually encountered in the dense CO₂ transportation system of CCS, while the latter may occur when an aqueous phase forms at the bottom of a dense CO₂ transportation pipeline (especially for upset conditions) or in down-hole material corrosion problems in the oil and gas industry. The corrosion of steel in a dense CO₂-saturated water phase with impurities will not be the main focus of this present work. The review of steel corrosion in supercritical CO₂ in nuclear systems and of CO₂ corrosion in oil and gas pipelines, for which the related articles can be easily found in the open literature [53–58], are also outside the scope of this work. CO₂ is not corrosive, and its carbonic acid that speciates *in situ* is the issue. CO₂ corrosion refers to the carbonic acid corrosion in this work.

Influential parameters and mechanisms

Impurities

Impurities are crucial parameters in causing and determining the extent of degradation of steels in dense CO₂. The quality recommendations for the CO₂ transportation provided by the DYNAMIS and EOR projects are shown in Table 3. If impurities can be completely removed from CO₂, corrosion will never be a concern in safe dense CO₂ pipeline transportation. However, no international consensus on the quality standards for the specification of CO₂ mixtures has yet been achieved for pipeline transmission systems [59], for either EOR or CCS purposes. Based on the degree of corrosion attack by combinations of contaminants, four regimes with different risks of pipeline integrity degradation were outlined for CCS dense CO₂ transportation by Cole et al. [7]:

- (i) Very low contaminant levels and extremely low water content.
- (ii) Low contaminant levels and water content below the solubility limit.
- (iii) Low contaminant levels and water content above the solubility limit.
- (iv) Moderate contaminant levels and water content above the solubility limit.

It has not yet been determined which regime will be followed in future CCS systems. Before establishing the criteria, corrosion issues must be addressed. A series of studies have followed the four regimes to study the corrosion risk of pipeline steels in dense CO₂ environments, and a number of them have shown that impurities such as SO₂, NO_x, H₂S, HCl, and O₂ exhibit remarkable effects on the corrosion rate of steel in the CO₂-rich phase [16,17,23,24,30–32,36–38,40–42,45,62–65]. The test conditions for steel corrosion in dense CO₂ with impurities to date are summarised in Appendix A, for convenient searching and citations. The separately summarised test conditions related to supercritical CO₂ corrosion can also be found in the works by Wei et al. [66], Barker et al. [67], and Hua et al. [13,28,29,32].

H₂O

The water content plays a critical and principal role on the corrosion behaviours of pipeline steels in dense CO₂

Table 3. DYNAMIS CO₂ quality recommendation compared to the existing CO₂ qualities for EOR purpose [1,59].

Component	DYNAMIS CO ₂ quality recommendation									
	Canyon Reef Carriers	Central Basin	Sheep Mountain	Bravo Dome	Cortez	NEJD	Sleipner	Weyburn	Concentration	Limitation
H ₂ O	50 ppm wt.	257 ppm wt.	129 ppm wt.	–	257 ppm wt.	–	Saturated	<20 ppm vol.	500 ppm	Design and operational considerations
H ₂ S	<200 ppm	<20 ppm (spec)	–	–	0.002%	Trace	<150 ppm	9000 ppm	200 ppm	Health and safety considerations
SO _x	–	–	–	–	–	–	–	–	100 ppm	Health and safety considerations
NO _x	–	–	–	–	–	–	–	–	100 ppm	Health and safety considerations
O ₂	–	<10 ppm wt (spec)	–	–	–	–	–	<50 ppm wt.	Aquifer <4 vol.-% (all non cond. gasses), EOR >100 ppm	Technical limit; storage issue
CO	–	–	–	–	–	–	–	1000	2000 ppm	Health and safety considerations
CH ₄	2–15% C ₆ H ₁₄	0.2%	1.7%	–	1–5%	Trace	Total hydrocarbons: 0.5–2.0%	0.7%	Aquifer <4 vol.-%, EOR <2 vol.-%	As proposed in ENCAP project
C ₂₊	–	–	0.3–0.6%	–	Trace	–	Total hydrocarbons: 0.5–2.0%	2.3%	–	–
N ₂	<0.5%	1.3%	0.6–0.9%	0.3%	4%	Trace	Non-condensable gases (N ₂ , H ₂ , Ar): 3–5%	<300 ppm	<4 vol.-% (all non-condensable gasses)	As proposed in ENCAP project
Ar	–	–	–	–	–	–	Non-condensable gases (N ₂ , H ₂ , Ar): 3–5%	–	<4 vol.-% (all non-condensable gasses)	As proposed in ENCAP project
H ₂	–	–	–	–	–	–	Non-condensable gases (N ₂ , H ₂ , Ar): 3–5%	–	<4 vol.-% (all non-condensable gasses)	Further reduction of H ₂ is recommended, because of its energy content
CO ₂	85–98%	98.5%	96.8–97.4%	99.7%	95%	98.7–99.4%	93–96%	96%	>95.5%	Balanced with other compounds in CO ₂

environments because the existence of water provides the basic conditions for electrolyte formation on the steel surface and further determines the extent of general and localised corrosion. Very strict limitations on the water content have been implemented for EOR CO₂ transportation, but the open literature still lacks the specifics of the dehydration process for the EOR CO₂ stream [6]. It has been found that the water content within each CO₂ stream for EOR projects varies from 20 to 630 ppm, with the exception of the Sleipner project, which transports CO₂ with saturated water using corrosion resistant alloy (CRA) pipelines [67].

A number of studies [1,10,27,28,35,39,68] have shown that when CO₂ is water-free or has relatively low moisture content, the corrosion rates of pipeline steel are zero or negligibly low. Field experience also indicates very few problems in relation to dry CO₂ transportation in carbon steel pipelines [69]. However, once CCS is applied on a large scale, it will be impossible to dry the dense CO₂ stream to a dew point well below the ambient temperature in all cases [70]. It has been estimated that with a less restricted water removal limit (increasing to 400 ppmv), the total cost for impurities removal per tonne of CO₂ will decrease by 50% of the cost for the more restricted removal (50 ppmv of water) for the case of a coal-fired plant [71].

Different water contents can lead to different phase state of water in dense CO₂. Water content below the solubility limit will lead to dissolved water in the bulk CO₂ stream, while water content above the solubility limit can lead to a condensed and segregated aqueous phase on the steel surface. Furthermore, the dissolved water and the condensed water in dense CO₂ have essentially different impacts on the corrosion behaviour of steel. When the water content in CO₂ exceeds the solubility limit, water molecules will cluster together to form a liquid and separate phase or the so-called condensed phase, which will further absorb CO₂ and other impurities (e.g. SO_x, NO_x, H₂S, HCl, and O₂), thus providing the aqueous environment required for electrochemical reactions. Conversely, when the moisture is very low, there will be no aqueous phase, thus resulting in an absence of electrochemical reactions. Obviously, it is more difficult for the electrolytes to form and for electrochemical reactions to occur in dense CO₂ with under-saturated water than in dense CO₂ with saturated water.

Thus, the solubility of water in high-pressure CO₂ is a critical issue for dense CO₂ corrosion, and it has been studied by a few researchers, including both experiment [72,73] and model studies [74,75]. However, the solubility of water in high-pressure CO₂ is believable to be considerably influenced by other impurities. Figure 1 illustrates the effect of CH₄ on lowering the water solubility limit in dense CO₂ [74]. The lines are the calculated results obtained with the Soave–Redlich–Kwong equation of state with the Huron–Vidal mixing rule (SRK–HV) model, and the points are experimental data from Song and Kobayashi [76]. A similar effect in terms of lowering water solubility limit was found for N₂ by Foltran et al. [77]. Similar effect of HCl on the solubility of water in dense CO₂ was also found by Cole et al. [78]. At present, very limited data relating to water solubility in impure CO₂ can be achieved; therefore, researchers have usually used the water solubility data in pure CO₂ to calculate the water content needed for the experiments, which will inevitably generate misjudgement on the phase state of water.

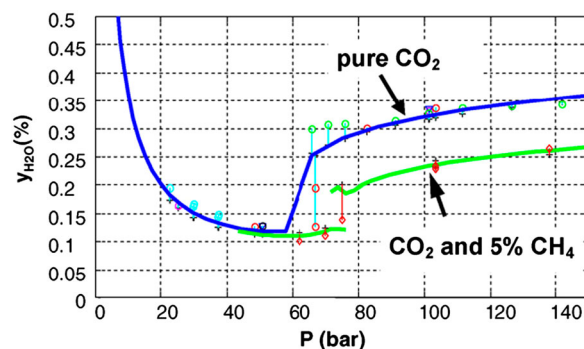


Figure 1. Water solubility in pure CO₂ and in a CO₂–CH₄ mixture at 25°C [74].

The general and localised corrosion problems of carbon steel in dense CO₂ are generally believed to become more severe when the water content increases [28]. Yevtushenko and Bäßler [79] illustrated that the corrosion rate increased when increasing the water content from 500 to 1000 ppmv in the flow loop test. However, in CORROSION/2014, Yevtushenko also reported that when they increased the water content from 1000 to 2000 ppmv, the corrosion rate decreased. They repeated the test and obtained the same result. The same interesting results were found by Thodla et al. [80], who also showed that when the water content was reduced from 1000 to 100 ppm, the corrosion rate increased. These interesting results still need thorough investigation. It is reasonable that Sim et al. [39] found that the corrosion rate did not change much with the addition of water, once the water content in the supercritical CO₂ reached saturation.

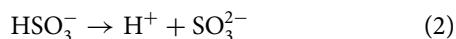
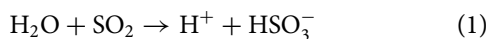
In addition to the effects of the water solubility limit on the corrosion behaviour, it was found that, similar to the circumstance of atmospheric corrosion [81], there exists a critical relative humidity (RH) in the supercritical CO₂ environment [39,46], above which the corrosion rate increases dramatically with increasing RH. RH (usually in units of %) is defined as the ratio of the actual water content and the water solubility limit and is another representation of the moisture degree in addition to the actual water content (usually in units of ppmv). The sharp increase in corrosion rate occurring at the critical RH is believed to be closely related to the change in corrosion mechanism, that is, the corrosion type is argued to change from chemical corrosion to electrochemical corrosion, since a thin water layer forms as RH increases [46].

For the case with very low RH, no continuous water layer forms, and the anodic process of corrosion will be suppressed along the hydration of the metal ion. The passivation of the anodic process is the main reason for the low corrosion rate under low RH conditions [82]. That is, in the case of RH below the critical RH, the corrosion process is mainly controlled by the anodic process, while for a higher RH, the corrosion process is subject to cathodic process control [82]. Although the study of corrosion in supercritical CO₂ with thin electrolyte layers can refer to a few new methods employed in atmospheric corrosion studies [83,84], the high-pressure environment restricts the employment of certain *in situ* technologies. Despite some research on electrochemical test technologies in the CO₂-rich phase [85,86], the use of electrochemical methods in supercritical CO₂ systems remains questionable and is not widely applied.

Overall, there is no consensus on the tolerable water content required for dense CO₂ transportation, either for a CO₂ stream with only SO₂ and H₂O or for a CO₂ stream with multiple impurities (SO_x, NO_x, H₂O, O₂, H₂S).

SO_x

SO_x stands for SO₂ and SO₃, and SO₂ can be oxidised to SO₃ by O₂. Dissolved SO₂ can ionise in two steps as follows [87]:



SO₂ was found to accelerate the corrosion rates when the SO₂ concentration increased [23,27,45,88]. The presence of SO₂ results in the formation of sulphurous acid by reacting with H₂O and further reacting with O₂ to form sulphuric acid in the aqueous phase, thus lowering the pH and providing more H⁺ ions to participate in and enhance the cathodic reactions. Although it remains unclear whether SO₂ first reacts with water in the bulk dense CO₂ phase to form acid, which then condenses onto the steel surface, or if a thin water layer first forms on the steel surface and then reacts with SO₂ and O₂, or if both of these processes co-exist in dense CO₂ systems. The general corrosion mechanism in dense CO₂ with SO₂ and H₂O has been suggested in detail by several authors [23,28,46].

When a relatively high concentration of SO₂ (for example, 2% mol) is present, the corrosion behaviour of steel in dense CO₂ is not dominated by CO₂ but by SO₂. Choi et al. [23] and Xiang et al. [45] found that when SO₂ was added to the supercritical CO₂ system, iron sulphite was the main corrosion product instead of FeCO₃. It is easy to understand that when SO₂ concentration is high, a high concentration of sulphurous acid will form in the condensates on the steel surface, and once FeCO₃ is formed, it will be dissolved by sulphurous acid. However, if the SO₂ concentration is extremely low, the amount of sulphurous acid cannot dissolve all the FeCO₃, resulting in a mixed and complex composition of corrosion products, thus enhancing the difficulty of product detection.

In terms of the interaction between SO₂ and H₂O, it was found that SO₂ concentration tends to lower the tolerable water content for avoiding pipeline corrosion in supercritical CO₂ transportation [30]. Hua et al. [30] found that the introduction of 50 ppm SO₂ and 20 ppm O₂ resulted in a significant reduction in the tolerable water content required to stay below a general corrosion rate of 0.1 mm/y, reducing it to ~2120 ppm, and further increasing the SO₂ content to 100 ppm reduced the critical water content to ~1850 ppm. They also noted that corrosion can occur with water content of 300 ppm, well below the solubility limit of water in supercritical CO₂, in the presence of 0, 50, and 100 ppm SO₂ [30]. Similar results were also reported by Dugstad et al. [89]. Therefore, the introduction of SO_x will inevitably increase the risk of pipeline integrity degradation by enhancing the extent of corrosion.

NO_x

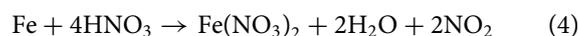
NO_x stands for NO and NO₂, and NO can be oxidised to NO₂ by O₂. Both NO and NO₂ were found to cause very severe corrosion issues in pipeline steels [90,91]. The presence of NO₂ leads to the formation of HNO₃ in the condensates,

which is an extremely strong acid with high causticity [92]:



HNO₃ has a similar accelerant effect on the corrosion behaviour of steel to HCl [22]. However, the diffusion ability of HNO₃ is higher than for HCl and H₂SO₄, which means it may more easily induce severe corrosion problems on the internal surface of supercritical CO₂ pipelines [37]. The neural network modelling results by Sim et al. [21] also showed that HNO₃ had the most notable impact on the corrosion rate of all the potential acids.

Another reason for the high corrosion rates in HNO₃ is derived from the rapid autocatalytic reduction of HNO₃, known as a strong oxidising agent [93]. The mechanism is explained as the primary displacement of hydrogen ions from the aqueous, which is followed by reduction of HNO₃ rather than hydrogen evolution since the acid reduction leads to a marked decrease in free energy [94]:



HNO₃ has a strong oxidation effect on Fe²⁺, leading to the formation of a rust-like dusty product, which was always fluffy and exhibited poor protection on the substrate, without the ability to efficiently reduce the corrosion rate [92]. A blackish/orange coloured dusty film was found forming on the X65 steel surface in wet supercritical CO₂ with NO₂ [63]. The composition of the products formed in a continuous flow of CO₂ containing NO₂, SO₂ and CO was found to be very complex [36].

HNO₃ was also found to increase the pitting potential in supercritical CO₂ [40] and to increase crevice corrosion susceptibility in aerated sea water under ambient pressure [95]. Furthermore, Sandana et al. [96] noted that nitrates might increase the susceptibility to stress corrosion cracking (SCC) in bicarbonate/carbonate environments. They suggested further experimental work to quantitatively assess the crack susceptibility at high CO₂ partial pressures.

Recently, Sun et al. [91] found that localised corrosion commonly existed in water-saturated supercritical CO₂ systems containing NO₂ with and without other impurities. They stated that NO₂ can greatly accelerate the separation of water from dense CO₂ fluids, and water droplets subsequently condense onto the steel surface, causing localised corrosion of the steel underneath the water droplets, with the spherical corrosion products right on top of the pits, as shown in Figure 2. From the pipeline integrity management perspective, NO_x should be removed most thoroughly, among all the acidic gas impurities, due to its detrimental effect on the pipeline integrity.

H₂S

When H₂S exists in dense CO₂, it can dissolve in the water layers and promote corrosion by affecting both the anodic and cathodic processes. Aqueous H₂S is a mild acid that can partially dissociate in two steps [97]:



Based on records of CO₂/H₂S corrosion in oil and gas industry, ignoring the cracking aspects of corrosion problems, H₂S can either enhance CO₂ corrosion by acting as a promoter of anodic dissolution through sulphide adsorption

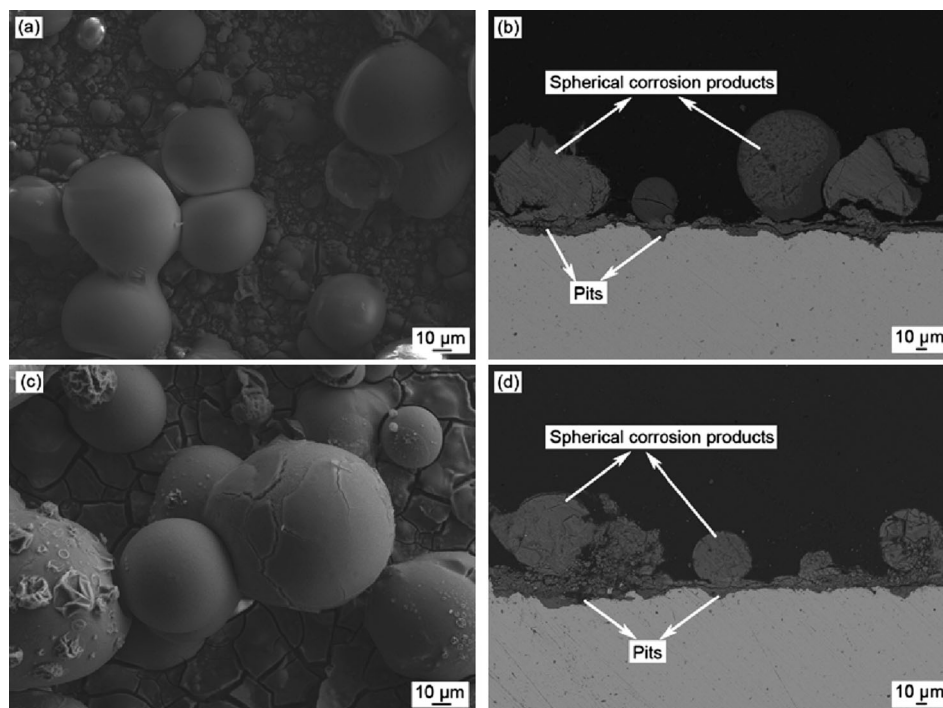


Figure 2. (a) and (c) SEM surface morphologies and (b) and (d) cross-sectional backscattered electron images of corrosion scales after corrosion for different time in water-saturated supercritical CO₂ system containing 1000 ppmv NO₂ at 10 MPa and 50°C: (a) and (b) 24 h and (c) and (d) 120 h [91].

and lowering the pH or reduce CO₂ corrosion by forming a protective sulphide scale [55]. The formation reaction of the corrosion products is the following solid-state reaction [98]:



Usually, the H₂S-induced corrosion is always highly localised (pitting or mesa-type attack). The formation of iron sulphide layers (such as mackinawite, pyrrhotite, and greigite) is related to the localised corrosion, and their physical properties and protectiveness vary with the conditions [99,100]. The electrode potential gradients created by the local galvanic cells between the iron sulphide and the uncovered area are believed to drive the localised corrosion [101].

Localised corrosion was found to be dominant for low alloy steels (P110 and 3Cr steel), while 316 L stainless steel was highly resistant to corrosion in the supercritical CO₂ phase with H₂S impurity [102]. Choi et al. [24] showed that the addition of 200 ppm H₂S in the supercritical CO₂ phase dramatically increased the corrosion rate of all tested materials (carbon steel, 1Cr and 3Cr steels) in CO₂ with saturated water. However, lowering the water content to 100 ppm in supercritical and liquid CO₂ with 200 ppm H₂S reduced the corrosion rate to less than 0.01 mm/y [24]. A small amount of H₂S was reported to change the adsorbability of H₂O onto the steel surface [42], causing the adsorption of H₂O on the whole steel surface, thus accelerating the general and localised corrosion of carbon steel in the supercritical CO₂ phase. Like nitrates, hydrogen sulphide can also cause internal SCC in CO₂ pipelines, which requires more consideration when the transported CO₂ contains H₂S.

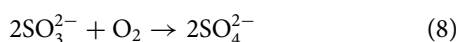
O₂

Oxygen will inevitably be encountered in the CO₂ stream in CCS systems that capture CO₂ from coal-fired plants, especially for the oxy-fuel capture technology. Dugstad

et al. [27] and Choi et al. [23] preliminarily studied the effect of O₂ content on the corrosion rate of pipeline steel in supercritical CO₂. It was previously believed that the presence of O₂ generally increased the corrosion rate. However, the experimental results by Hua et al. [31] revealed that increasing the O₂ concentration from 0 to 1000 ppm caused a progressive decrease in the general corrosion rates of X65 and 5Cr steel in water-saturated supercritical CO₂ but tended to increase the extent of localised corrosion observed on both materials. Additionally, Zeng et al. [103] concluded that the influence of oxygen on corrosion is related to the existence of water and the CO₂ stream pressure, and there is a threshold pressure (~10 MPa) of a supercritical CO₂ stream containing water and oxygen, above which the corrosion rates of pipeline steels become noticeable. Ayello et al. [104] found that a small amount (100 ppm) of O₂ had essentially no impact on the corrosion rate of steel in supercritical CO₂. Xu et al. [105] found that high O₂ concentrations exerted no influence on uniform corrosion rates of X70 steel in supercritical CO₂ at a relative water content of 45%, enhanced the general corrosion at a relative water content of 50–60% and localised corrosion at a relative water content of 50–88%, but decreased the general corrosion at a relative water content of 75–100% and localised corrosion at a relative water content of 100%. They also found that the addition of O₂ decreased the tolerable water content of the transport system. These controversial results imply that more corrosion experiments related to different amounts of O₂ in dense CO₂ are needed to reveal the complex effects of O₂ on corrosion behaviours, especially under conditions of multiple impurities.

When O₂ is the only gas impurity in a normal-pressure CO₂ system, it will induce the formation of porous iron oxides with low protectiveness and inhibit the formation of a protective FeCO₃ film, resulting in poor protectiveness of the product scales [106], which will eventually induce localised corrosion. It was proven that increasing the O₂ content in water-saturated CO₂ in the presence of X65 and 5Cr

suppressed the growth of iron carbonate (FeCO_3) on the steel surface and resulted in the formation of a corrosion product consisting mainly of iron oxide (Fe_2O_3) [31]. When SO_2 and O_2 co-exist in the CO_2 system as gas impurities, O_2 can react with water and SO_2 to form sulphuric acid, which is more corrosive than sulphurous acid. O_2 can also provide more depolarising agents to the cathodic reactions [107,108] and oxidise SO_3^{2-} in the following reaction [109]:



Other impurities

HCl can exist in the CO_2 stream, especially for CO_2 captured from the flue gas of biomass boilers. According to Cole et al. [78], the addition of HCl decreases the solubility of water in CO_2 so that the mass of the aqueous phase progressively increases with increasing HCl. They presumably concluded that the increasing ionic nature of the water content is the cause of the decrease in solubility in the carbon dioxide phase. Another study by Ruhl and Kranzmann [37] found that both apparently amorphous and angular corrosion products were found on samples immersed in supercritical CO_2 with HCl and H_2O impurities, and the crystalline structures appeared hollow at higher magnifications, indicating that the scales could not provide much protection to the substrate.

The existence of HCl will also introduce another problem: the introduction of Cl^- . At room temperature, Cl^- ions may have an inhibitory effect on CO_2 corrosion [110]; however, at high temperature, Cl^- ions may cause localised corrosion of the alloy steel. In contrast, Gao et al. [111] argued that localised corrosion of X65 steel in a CO_2 aqueous environment under ambient pressure could be initiated by changing the solubility of iron carbonate and the subsequent changes in the ionic strength of the solution, which was not directly caused by high Cl^- concentration.

For pre-combustion technology, CO will inevitably exist in the captured CO_2 . CO has a similar effect as NO_x , which can induce an SCC problem that has been observed for approximately 40 years in CO_2 -CO- H_2O environments, with the partial pressure of CO_2 below 2.0 MPa [96]. For high-pressure conditions in dense CO_2 , the task of elucidating this issue remains. No evidence currently exists to show that CO can promote or depress general corrosion or induce localised corrosion in dense CO_2 environments.

Since most of the CO_2 is captured by organic amines, it is possible that organic amines will be present in the CO_2 stream. The results of Thodla et al. [80] indicated that the presence of monoethanolamine (MEA) decreased the corrosion rate, while Collier et al. [26] found that the presence of diethanolamine (DEA) increased the corrosion rate. MEA might serve as an inhibitor, adsorbing on the steel surface [4], while DEA might provide cathodic depolarising agents.

The presence of acidic gases markedly affects the pH value of the liquid film on the steel surface under supercritical CO_2 environments, by forming strong acids. They thereby result in more H^+ ions for the hydrogen evolution cathodic reaction, thereby increasing the corrosion rates. Cole et al. [78] found that at the minimum level of HCl contamination (2 ppm), the pH of condensates falls below 1.5 under both liquid and supercritical CO_2 conditions. The research results of CO_2 corrosion in the oil and gas industry showed that pH

had a significant impact on the corrosion behaviour of mild steel. It can influence both the electrochemical reactions that lead to iron dissolution and the precipitation of protective scales which governs the various transport phenomena associated with the former [55]. The corrosion mechanisms could be related to the changes of localised pH; however, this issue has not been addressed yet in the supercritical CO_2 environment by the experimental study. A mechanistic prediction model for supercritical CO_2 - SO_2 - O_2 - H_2O corrosion by Xiang et al. [19] showed that the localised pH on the steel surface increased due to the depletion of H^+ ions and the accumulation of HSO_3^- and SO_3^{2-} .

The hydrogen-induced cracking (HIC) have to be considered when an aqueous phase and impurities such as H_2S and NO_x exist. The threat and mitigation of HIC and SCC must be addressed in future standards related to the design and construction of pipelines for anthropogenic CO_2 transportation.

Pressure

Pressure herein includes the total pressure, the partial pressure of CO_2 , the partial pressure of O_2 and other gas impurities. Experimental results on CO_2 corrosion in the oil and gas industry showed that there was almost a linear growth relationship between the CO_2 partial pressure and the corrosion rate of pipeline steel at low CO_2 partial pressure [112]. For dense CO_2 environments with impurities, CO_2 becomes the solvent and the impurities become the solutes, making the CO_2 partial pressure substantially equal to the total pressure of the mixtures. Changing the total pressure can change the bulk phase state (gas, liquid, or supercritical), the total amount of corrosive medium, the solubility of impurities in the bulk phase, the morphology, and the properties of the product layers, thus influencing the corrosion behaviour of the pipeline steel. Changing the partial pressure of the impurity is equivalent to changing the concentration of impurity.

Choi and Nescic [25] preliminarily studied the effect of total pressure on the corrosion rate of X65 steel in a high-pressure CO_2 environment with saturated water, and the experimental results revealed that the corrosion rate increased when the total pressure increased from 6.0 to 8.0 MPa, with the CO_2 phase changing from gas to a supercritical state. Moreover, the increase in O_2 partial pressure can also generally increase the corrosion rate in a supercritical CO_2 system; however, the corrosion rate reaches a maximum value at 3.3 bar O_2 [23]. Meanwhile, increasing the partial pressure of SO_2 , which means increasing the SO_2 concentration, can also dramatically increase the corrosion rate of X70 steel and iron in a supercritical CO_2 system [45]. Recently, the results by Xu et al. [113] showed that the corrosion rates of pipeline steels at 8 MPa are higher than at 10 MPa when the water concentration is below 3000 ppmv, while the situation is the opposite when the water content was 3000 ppmv. They also found that the pitting rates were high, especially for the cases with 3000 ppmv water concentration.

The experimental data at higher total pressures are sparse, especially for the pressure more than 20 MPa. It has to be mentioned that for the high pressure environment, the non-ideality of gases will play an important role [55]. Instead of the CO_2 partial pressure, the CO_2 fugacity should be used

[114]. Since Henry's law can only be used in diluted solutions, non-ideal equilibrium models must be applied to precisely predict the solubility of the impurities in the condensed phase under high-pressure condition.

Temperature

The temperature in a dense CO₂ transportation system can vary from -56.7 to above 31°C, with the CO₂ phase changing from liquid to supercritical, based on the CO₂ phase diagram. Temperature is an operating parameter as critical as pressure, since it can affect the corrosion behaviour in many ways. It can affect the solubility product of FeCO₃ according to the following equation [115]:

$$\log K_{sp} = -59.3498 - 0.041377T_k - \frac{2.1963}{T_k} + 24.5724 \log(T_k) + 2.518I^{0.5} - 0.657I \quad (9)$$

where K_{sp} is the solubility product of FeCO₃, T_k is the temperature in Kelvin and I is the ionic strength of the solution.

In addition to the effect on the bulk phase, temperature directly influences the exchange current density, chemical reaction equilibrium constants, chemical reaction rate constants, fluid viscosity, and fluid density. Moreover, temperature can affect the morphology and properties of product layers and the component diffusion coefficients, thus indirectly influencing the corrosion behaviours.

Notwithstanding, the corrosion rates of X70 steel in supercritical CO₂ mixtures first increased with temperature, reaching a peak value near 75°C, and then decreased with temperature [43,48], which showed a similar influence trend of temperature on the corrosion rate of pipeline steel in a low partial pressure CO₂ environment [116]. The effect

of temperature on increasing the corrosion rates of pipeline steel in supercritical CO₂ compared with liquid CO₂ was suggested by several researchers [27,43]. In contrast, Ruhl and Kranzmann [36] found that the corrosion rates became more pronounced with decreasing temperature and increasing humidity, though the tests were under ambient pressure instead of high pressure. Meanwhile, Hua et al. [28] revealed that the corrosion rate of X65 steel increased as the temperature decreased from 50 to 35°C when the water content was lower than 1600 ppm (mol). These paradoxical experimental results require deep investigations to explain.

It is noteworthy that temperature has a great impact on the surface morphology of corroded samples, as shown in Figure 3, further affects the protectiveness of product layers, thus eventually determining the general and localised corrosion. Under supercritical CO₂ conditions, the porosity test results of the product scales indicated that the loose product layer with poor protectiveness was related to low temperature, while a more compact product layer with better protectiveness was related to high temperature [43].

Flow

CO₂ corrosion studies for low partial pressure conditions have shown that the increase in flow velocity would usually increase the corrosion rate, which derives from accelerating the speed with which the depolarising agent reaches the sample surface to participate in the electrode reaction, i.e. enhancing the cathodic depolarisation process and accelerating the transfer rate for the reaction products to move away from the steel surface, thus eventually enhancing the corrosion process [112]. However, after the formation of the corrosion product layers, the impact of flow velocity on the corrosion rate was found to be weakened [117],

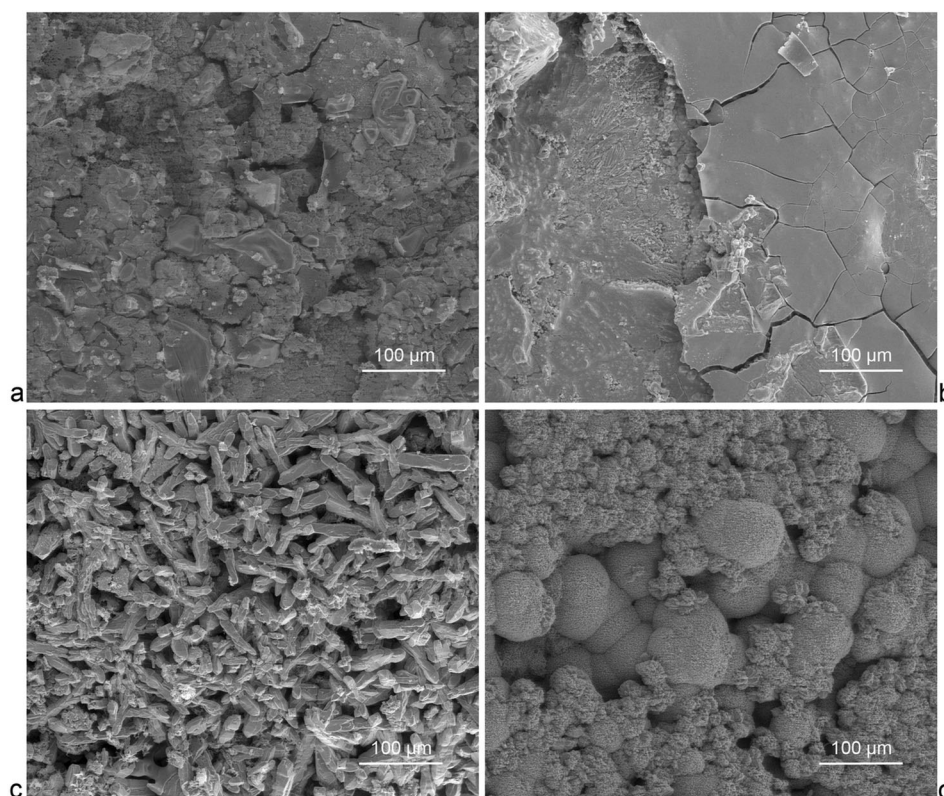


Figure 3. Surface morphology of X70 steel in supercritical CO₂ mixtures (10 MPa, 120 h, 5 g H₂O, 0.02 mol O₂ and 2% mol SO₂) changes with temperature [43]. (a) 298 K; (b) 323 K; (c) 348 K; (d) 366 K.

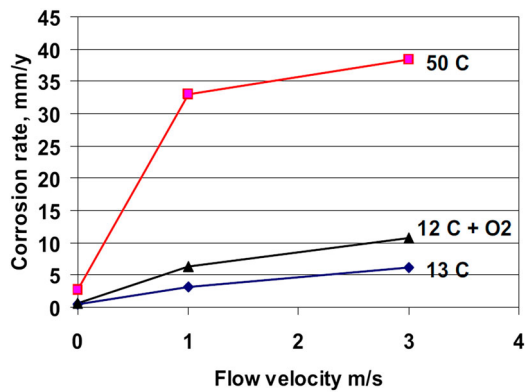


Figure 4. Corrosion rate as a function of flow velocity in dense CO₂ (10 MPa) [27].

which may be related to the greatly diminished flow velocity by porous corrosion product layers. It is noted that the flow shear stress near the pipeline wall might also affect the formation and stability of the product layer and inhibitor film [55], though the recent results by Li et al. [118] revealed that the mechanical removal of an FeCO₃ layer solely by wall shear stress, typically observed in multiphase flow lines, is highly unlikely under ambient pressure. Moreover, the flow regime may have great impact on the pipeline internal corrosion in dense CO₂, which implies that the desired properties of CO₂ should be adequately monitored to avoid the phase changes and ensure the maintenance of a single-phase flow throughout the pipelines [119]. Furthermore, flow-induced localised corrosion and erosion problems in the presence of particulates may also occur in dense CO₂ environments.

To date, sparse studies with relevance to the flow effect under a dense phase CO₂ environment have been conducted in closed autoclave systems. The work by Dugstad et al. [27] revealed that in supercritical CO₂ at 50°C, the corrosion rate of X65 steel at a flow velocity of 3 m s⁻¹ condition was approximately 10 times the value with no flow, as shown in Figure 4. The similar effect of the flow on the corrosion rate was also found in liquid CO₂ [27]. In contrast, the work by Farelas et al. [120] revealed that a 1000 rev min⁻¹ rotating speed in the autoclave can depress the corrosion rate of X65 in the supercritical CO₂ system distinctly. Hua et al. [32] stated that the flow can reduce the amount of water condensing onto the sample surface, thereby depressing the corrosion.

Meanwhile, only a few of the existing supercritical CO₂ corrosion tests were completed in the flow loop [79,121], and the test results in the flow loop were believed to show better reliability than the test results obtained in the sealed autoclaves. There is no doubt that more studies under different flow conditions in the flow loop are needed, especially for multiphase flow conditions in the CO₂ pipeline with different flow regimes, which may represent a gas-liquid flow in the worst-case scenario. The gas-liquid flow could be encountered when the pressure was reduced due to CO₂ pipeline rupture or other disrupted conditions.

Exposure time

A number of tests by different researchers have shown that, as the corrosion reactions proceeded, the corrosion products

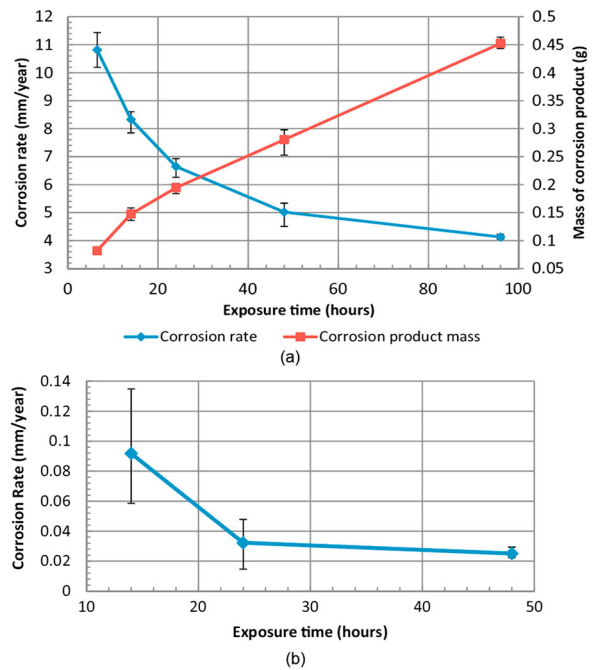


Figure 5. Corrosion rate and corrosion product mass of X65 carbon steel as a function of exposure time in: (a) supercritical CO₂-saturated water; (b) water-saturated supercritical CO₂ (8 MPa and 50°C) [29].

gradually accumulated on the sample surface, thickening the corrosion product layers with exposure time [15], both in a supercritical CO₂-saturated water phase and a water-saturated supercritical CO₂ phase, as shown in Figure 5 [29]. As the exposure time extended, the mass of corrosion product layers increased and the corrosion rate decreased, which suggested that the presence of the corrosion product layers effectively protected the substrate metal and reduced the corrosion rate. In a 454 h test conducted by Xiang et al. [44], the pitting corrosion beneath the product layers was highlighted as a serious problem.

Notably, the autoclave test method was employed in most studies. Since the autoclave is a closed system, the corrosive species will be gradually consumed, decreasing the corrosive species concentrations, which might contribute to the decrease in corrosion rates with exposure time. This issue was first mentioned by Xiang et al. [15] in the supercritical CO₂ environment, then elaborated in detail by Hua et al. [30] and Barker et al. [67]. If the impurity concentrations are high enough to make up for the consumption of corrosion reaction, the impact of decreasing the impurity concentration is limited. When the impurity concentration is low, the impact of the consumption of impurities on the corrosion rate might not be discounted. Brown et al. [62] claimed that a large portion of the corrosive phase can be trapped in dead legs or wet the autoclave walls preferentially. They also noted that the interaction of impurities in the bulk phase was another reason for the decrease of the active corrosion phase concentrations [62].

A system with impurity replenishment was another method to diminish the effect of decreasing the impurity concentration, which was employed by Yevtushenko and Bäßler to test the corrosion behaviour of steel in supercritical CO₂ [79]. A rocking autoclave with an impurity replenishing system and venting lines for CO₂ composition online analyses was also employed for dense CO₂ corrosion

studies to overcome the shortcomings of the impurity consumption [89].

Product layers

In CO₂ corrosion, if a protective layer forms on the steel surface, a diffusion process controlled by the product layer may become the rate-determining step (RDS) in the corrosion process [122]. Four characteristics are generally used to judge the protectiveness of the product layer: layer density, adhesion, stability, and surface coverage [55].

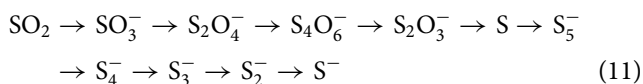
To date, there have been limited studies on the formation mechanisms of the product layer in supercritical CO₂ environments with impurities and their properties, while studies related to the FeCO₃ layer formation in supercritical CO₂-saturated water environments have been performed in detail [14,29]. If the supersaturation exceeds the solubility of FeCO₃ in the solution, FeCO₃ will precipitate on the steel surface.

In a supercritical CO₂-saturated water environment, the mechanical properties of the FeCO₃ layer and the relationship between the corrosion rate and the fracture toughness, as shown in Equation (10), were proposed by Zhang et al. [14] as follows:

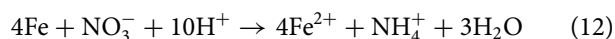
$$CR = \frac{3.25}{K_{IC}^{3/2}} - 0.908 \quad (10)$$

Another study conducted by Hua et al. [29] indicated that the FeCO₃ layer formed in a supercritical CO₂-saturated water environment consisted of two layers: the loose amorphous FeCO₃ inner layer and the compact FeCO₃ crystal outer layer. However, the localised corrosion rates were still high, even though the layers seemed to be compact, in water-saturated supercritical CO₂.

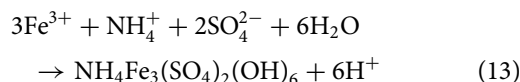
The composition of the product layer and the effect on corrosion behaviour become more complicated when the acidic gases are contained in a dense CO₂ stream. Taking SO₂ as an example, FeSO₃·xH₂O and FeSO₄·xH₂O crystals are usually detected in the product layers [46], while FeCO₃ cannot be found in the product unless the SO₂ concentration in the corrosion environment is fairly low [32]. A mixed product layer containing FeSO₃·3H₂O and FeCO₃ was found under conditions of 50 and 100 ppm SO₂ and 20 ppm O₂, and the ratio of FeSO₃·3H₂O to FeCO₃ increased with increasing SO₂ concentration [32]. Moreover, Ruhl and Kranzmann [38] suggested that the inner part of the FeSO₃·xH₂O and FeSO₄·xH₂O layers changed to iron sulphide (FeS) under ambient pressure. The changing process was characterised by the following equation [123]:



When NO_x and SO_x were present, ammoniojarosite ((NH₄)Fe₃(SO₄)₂(OH)₆) was found to be the main corrosion product under ambient conditions [36], while Fe(NO₃)₃·9H₂O and Fe₂O₃·H₂O were detected as the main corrosion products for X65 steel in water-saturated supercritical CO₂ with 1000 ppmv NO₂ [91]. NO₃⁻ present in the solution might be reduced to ammonium (NH₄⁺) within the aqueous film and in the presence of hydronium ions (H₃O⁺) [37], according to the following equation [124]:

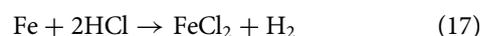
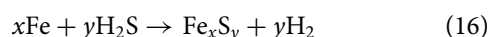
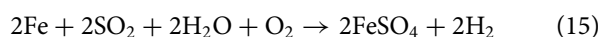


Ammoniojarosite ((NH₄)Fe₃(SO₄)₂(OH)₆) formed according to [125]:



For the case with SO₂, H₂S, and O₂ impurities, the complex product has been identified by Sun et al. [16], while for the case with NO_x, SO_x, H₂S, O₂, and HCl coexisting, there is still no experimental result that can be cited here to clearly show the exact composition of the product layers.

The following equations describe the other potential corrosion products of mild steel in the supercritical CO₂ environments:



A protective corrosion product layer, on the one hand, tends to reduce the flux of corrosive media reaching the metal surface, and on the other hand, may directly isolate part of the substrate metal from the corrosive media completely, thus substantially lowering the corrosion rate. Vitse and Nestic proposed the concept of surface coverage to describe the ability of the product layer to isolate the steel from the corrosive media [126].

The mechanisms of product layer formation under different conditions also need to be specified. Sun et al. [41] speculated the mechanisms of water layer and product layer formation for a water-saturated supercritical CO₂ system with O₂ and H₂S impurities, as shown in Figure 6. The exact product compositions and structures might be affected by impurity types and concentrations and the surface roughness of the inner wall of the CO₂ pipeline. Xu et al. [47] found that the initial surface roughness has no influence on the corrosion rate at a RH of <55% (45, 50, and 55%) and >88% (88, 100%). However, a rougher surface leads to higher corrosion rate at a RH between 60 and 75%.

Steel chemistry

The metallurgical variables (composition, heat treatment, and microstructure) play important roles in the corrosion of steels in dense CO₂ environments. Russick et al. [127] showed that carbon steel suffered corrosion problems in water-saturated supercritical CO₂, while 316 SS and 304L SS are corrosion resistant in the same environment. Hua et al. [31] found that when O₂ is present in water-saturated supercritical CO₂, 5Cr offers more resistance to pitting corrosion than X65 steel. They also found that with a concentration of O₂ above 500 ppm, the general corrosion rate of 5Cr steel was less than 0.04 mm/y, half the value measured for X65 steel [31]. However, the experimental results by Choi et al. [23] showed that the corrosion rates of X65 steel and 13Cr steel showed no outstanding differences in water-saturated supercritical CO₂ with SO₂ and O₂ impurities, revealing that 13Cr steel does not show higher corrosion resistance in the water-saturated dense CO₂ environment with SO₂ and O₂. Yevtushenko and Bäbler [79] also found that X20Cr13 steel showed severe pitting problems in supercritical CO₂ with H₂O, SO₂,

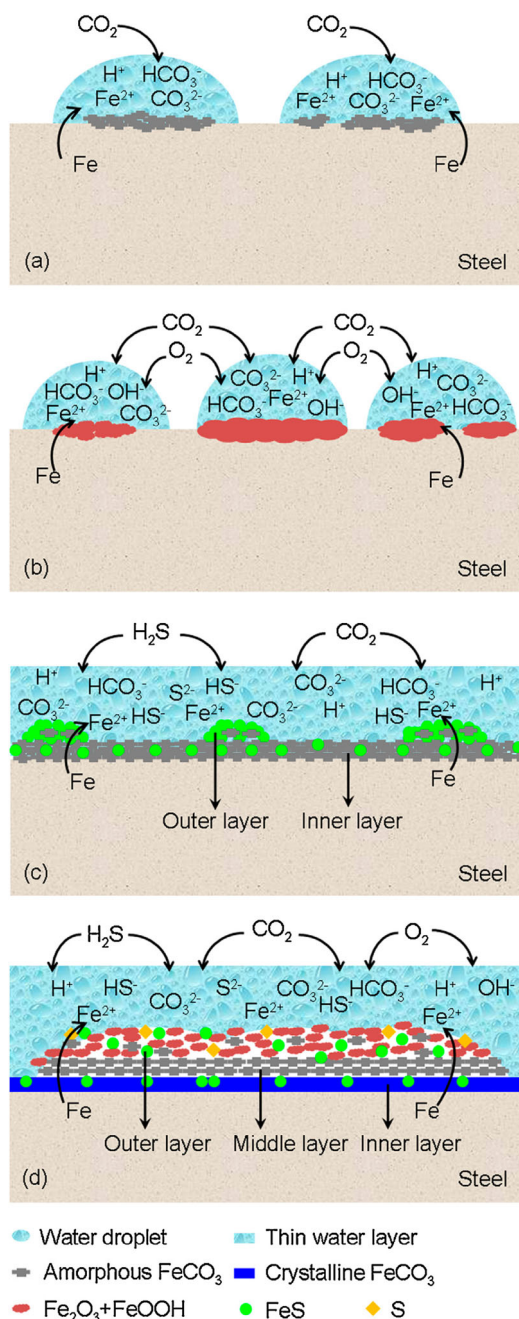


Figure 6. Schematic diagram of the corrosion of X65 steel in water-saturated supercritical CO₂ system: (a) CO₂-H₂O system; (b) CO₂-H₂O-O₂ system; (c) CO₂-H₂O-H₂S system and (d) CO₂-H₂O-O₂-H₂S system [41].

NO, CO, and O₂ impurities. Dugstad et al. [64] even found that high concentrations (>1000 mg L⁻¹) of Ni, Mo, and Cr were dissolved in the greenish liquid after corrosion testing, which indicated that the Hastelloy C autoclave was attacked in liquid CO₂ with H₂O, SO₂, NO₂, H₂S, and O₂ impurities.

It was indicated that the ions generated from the pipeline steel alloy elements, such as Mn²⁺, would be a catalyst to accelerate the oxidation reaction of SO₃²⁻ to SO₄²⁻. The differences between the physical properties of the FeSO₃ hydrate and the FeSO₄ hydrate products, such as the different solubility in water, may indirectly affect the corrosion process. However, the roles of other alloying elements in the corrosion of steels remain unknown in dense CO₂ with acidic gas impurities.

The effect of heat treatment on the corrosion behaviour of stainless steels during CO₂-sequestration into a saline aquifer was investigated by Pfennig et al. [8]. Low corrosion

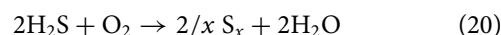
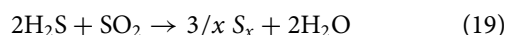
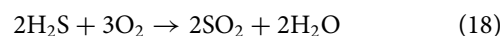
rates were obtained for steels with martensitic microstructures exposed to supercritical CO₂ at 100 bar, whereas normalised steels showed better corrosion resistance at ambient pressure [8].

Discussion of corrosion mechanisms

Synergistic effect

NO₂ and SO₂ were reported to have a synergistic effect that can intensify atmospheric corrosion, and moreover NO₂ had a catalytic effect on corrosion reactions [128]. Recently, Sun et al. [16] found that the synergistic effect of O₂, H₂S, and SO₂ impurities on the corrosion behaviour of X65 steel in water-saturated supercritical CO₂ systems was remarkable. Weight-loss tests revealed that the synergistic effect of multiple impurities significantly increased the corrosion rate of X65 steel. The complicated synergistic effects among CO₂, O₂, H₂S, and SO₂ resulted in the highest corrosion rate, as shown in Figure 7 [16]. The corrosion scales consisted of FeOOH, FeSO₃·2H₂O, FeSO₄·4H₂O, FeS, FeCO₃, and S [16], which implied a complex corrosion mechanism. The weak protective ability of the product scale might be one of the reasons for the synergistic increase in the effect of impurities on the corrosion rates.

The interactions among the impurities in the bulk phase have also attracted attention. Dugstad et al. [89] found that there was some elemental sulphur in the autoclave after the test for steel corrosion in supercritical CO₂ containing NO₂, SO₂, H₂O, H₂S, and O₂. The initiation of pitting corrosion by the presence of sulphur in a CO₂ environment has been reported by Fang et al. [129], which indicates that sulphur-initiated pitting may also occur in a supercritical CO₂ environment. Although the mechanism of sulphur formation is elusive, Dugstad et al. [89] speculated that the following reactions might occur:



Brown et al. [62] also suggested a similar reaction mechanism to Equation (20) between H₂S and O₂ at very low H₂S and O₂ concentrations. The formation of sulphur will lead to a

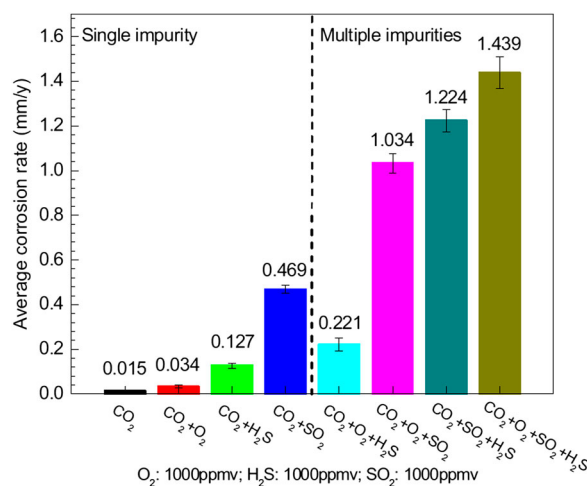
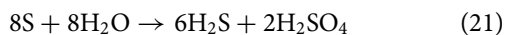
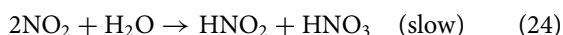
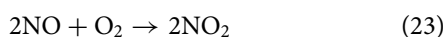
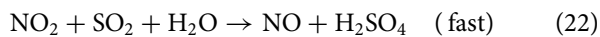


Figure 7. Corrosion rate of X65 steel exposed to water-saturated supercritical CO₂ containing various impurities (10 MPa, 50°C, 120 h) [16].

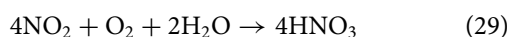
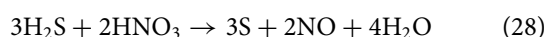
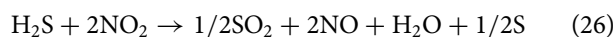
sulphur sedimentation problem that may block the pipelines and affect the accuracy of the electrical resistance electrode. Then elemental sulphur can react with H₂O to produce H₂S and sulphuric acid [130]:



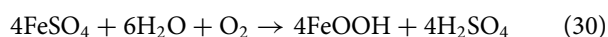
Dugstad et al. [89] also discussed the interaction between NO₂ and SO₂, that is, when NO₂, SO₂, O₂, and H₂O are present, SO₂ will be catalytically oxidised to H₂SO₄ by NO₂ (Lead Chamber Process) [131]:



More possible cross chemical reactions between impurities and their corresponding acids were proposed by Dugstad et al. [64]:



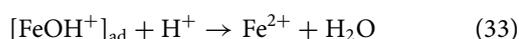
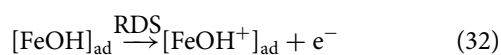
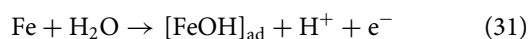
For the case with SO₂, O₂, and H₂O impurities, the ferrous sulphate product formed at anodic sites oxidises to ferric sulphate which in turn hydrolyses to produce iron oxyhydroxide, with the generation of sulphuric acid; the overall reaction is [132]:



To date, there is no open published model that can predict which of the above reactions are thermodynamically and kinetically possible and favourable under supercritical CO₂ test conditions, though an online measurement system was applied to determine the consumption rate of impurities in dense CO₂ [64]. However, the existing work offers some important information about the impurity interactions in the dense CO₂ phase.

Anodic and cathodic reactions

In addition to the bulk phase reactions among the impurities, the electrochemical reactions on the steel surface are the crucial steps in corrosion processes. The widely accepted anodic dissolution of iron in strong acid is the Bockris mechanism (BDD) [133]:

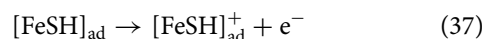
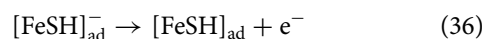
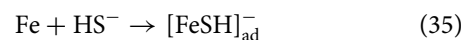


The total anodic reaction is as follows:



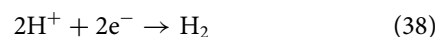
The above total anodic reaction is pH dependent in acidic solutions, with a typical measured Tafel slope of 40 mV [56]. This description can be applied where H₂S is not present in the system. In the presence of H₂S, the iron dissolution

mechanism can be expressed as follows [134]:

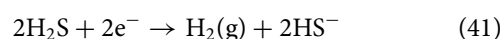
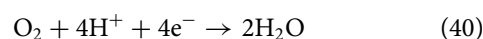


The question remains whether the anodic dissolution mechanisms of iron in dense CO₂ are consistent with the iron dissolution mechanism under low partial pressure conditions. In particular, when acidic gas impurities exist, the synergistic effect of impurities on the anodic dissolution mechanism is elusive.

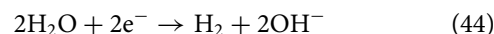
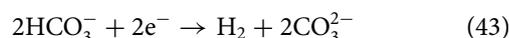
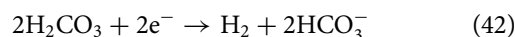
For the cathodic reactions, the most important confirmed reaction is the hydrogen evolution process:



The following cathodic reactions are also possible for the ingress of impurities [97,107,135]:



Due to the low pH conditions in dense CO₂ with acidic gas impurities, it seems that the following cathodic reactions that occur in low partial pressure CO₂ corrosion may not occur here:



Currently, no research has clearly illustrated the exact reactions of the cathodic processes. Other possible reactions might occur under the synergistic effect of impurities. The lack of research on the anodic and cathodic corrosion mechanisms is partly because of the limited methods of investigating corrosion mechanisms that can be applied to the dense CO₂ environment. Conducting electrochemical experiments in the aqueous phase saturated with supercritical CO₂ is expected to be helpful for investigating the corrosion mechanisms. Meanwhile, electrochemical investigation under ambient pressure might also be useful and valuable to provide some insight into the corrosion mechanism under high pressure. Tang et al. [86] recently developed a setup for *in situ* electrochemical measurements in H₂O-saturated supercritical CO₂ phase by using Ag/AgCl reference electrode, as illustrated in Figure 8. Their work is creative and the setup could be further used to investigate the cathodic and anodic corrosion mechanisms of steel in dense CO₂ phase.

Localised corrosion

For traditional CO₂ corrosion, localised corrosion is a common concern, in addition to general corrosion. A similar localised corrosion problem also occurs in dense CO₂ corrosion, even without acidic gas impurities and with high enough water content [30,62]. Most of the current published works focus on the general corrosion behaviour and mechanism of carbon steel, while few of them focus on localised corrosion issues. Moreover, most of the literature reports that mention the localised corrosion issue only note that the samples

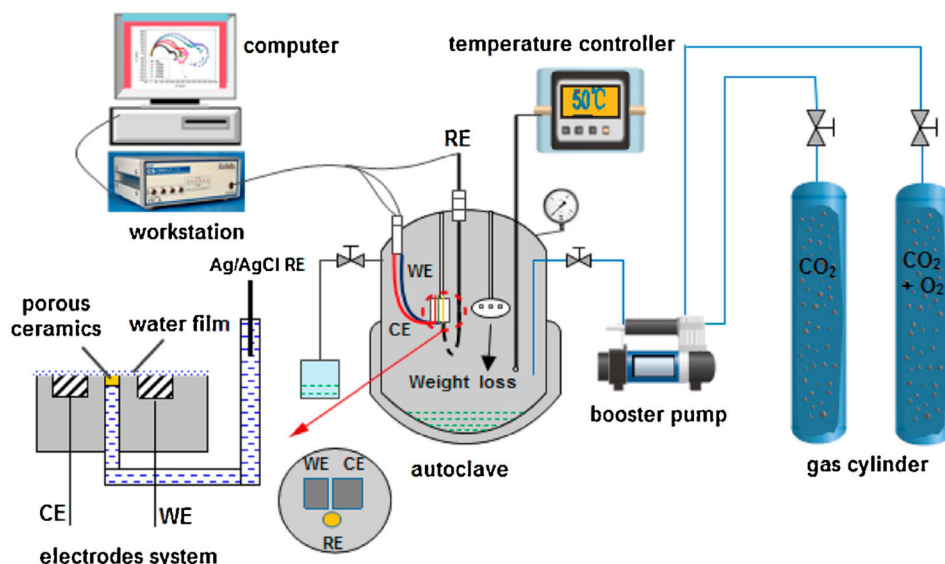


Figure 8. Schematic diagram of the setup for *in situ* electrochemical measurements in H₂O-saturated supercritical CO₂ environment [86].

encountered localised attack or that visible pitting regions were found on the sample surface, and the penetration rates were seldom determined.

Actually, localised corrosion is one of the serious threats to pipeline integrity in dense CO₂ transportation, as well as SCC and HIC. Localised corrosion also has a great impact on determining the upper limit of water content to avoid corrosion. The work of Xiang et al. [46] established a systematic method to determine the upper limit of water content for dense CO₂ pipeline transportation, by considering both the control of the general corrosion rate and the temperature variation of the fluids inside the pipes. However, Hua et al. [30] noted that the impact of localised corrosion should also be considered, and the authors concluded that the critical water content required to minimise the significant level of localised attack was substantially lower than the value required to prevent general corrosion (0.1 mm/y) and was determined to be approximately 500 ppm, regardless of SO₂ content (0, 50, or 100 ppm). When other impurities exist, such as NO_x, HCl, and H₂S, this estimated tolerable water content needs to be re-evaluated.

Barker et al. [67] discussed a series of fundamental questions relating to the localised corrosion of steel in dense CO₂. They suggested the investigation of the initiation, propagation, and stability of pits in a dense CO₂ environment to verify whether they would be the real threat to long-term operation in the field [67]. Currently, there is no literature identifying whether the pits are stable and continue to propagate, and the propagation kinetics also needs further investigation.

Sun et al. [91] recently found that the pits lie right under the spherical corrosion products in water-saturated supercritical CO₂ with NO₂ impurity, and other investigators have also shown localised corrosion under iron sulphate deposits in water-saturated dense CO₂ with SO₂ and O₂ impurities [44]. The localised penetration rates under the corrosion product were much higher than the general corrosion rates. It is essential to investigate the evolution rules of the corrosion products on the sample surface and their relation to the initiation and propagation of pits in dense CO₂ environments.

Mechanism differences for different CO₂ phase conditions

The corrosion mechanism differences between low partial pressure and supercritical condition (aqueous phase) have been studied by Zhang et al. [18]. They found that under both low CO₂ partial pressure and supercritical CO₂ condition, the corrosion behaviours of X65 steel, including characteristics of CO₂ corrosion product scale and the variation rule of corrosion rate with temperature, were similar. They concluded that the change in CO₂ partial pressure does not change the corrosion mechanism. They also explained that the corrosion rate was enhanced under supercritical CO₂ condition due to the higher carbonic acid concentration. Zhang et al. [136] stated that there was no essential difference in the electrochemical corrosion mechanism under supercritical CO₂ and non-supercritical CO₂ environments for the N80 steel in the aqueous phase.

Actually, corrosion in CO₂ environments can be divided into six circumstances: corrosion in aqueous phase with low CO₂ partial pressure (gas CO₂), wet gas phase with low CO₂ partial pressure (gas CO₂), aqueous phase with high CO₂ partial pressure (liquid CO₂), liquid CO₂ phase, aqueous phase with high CO₂ partial pressure (supercritical CO₂), and supercritical CO₂ phase. When the phase state of CO₂ is changed, the corresponding parameters (solubility, diffusion coefficient, viscosity, ionic strength, etc.) will change. With the presence of acidic gas impurities (SO₂, NO₂, H₂S, etc.), the corrosion mechanism will be thoroughly altered. The carbonic acid corrosion will change to sulphurous acid corrosion, nitric acid corrosion, and H₂S corrosion, or a mixed type of them. The corrosion products will also vary for different acidic gas impurities, which will affect the corrosion process in turn. For the corrosion in the dense CO₂ phase, the corrosion happened in the confined aqueous phase (water film), which is apparently different from the corrosion in the bulk aqueous phase. This characteristic has notable impact on the mass transport of species, and also affects the solubility of corrosion products, which will eventually affect the protectiveness of product layers to the substrate. The investigations on the effects of multiple acidic gas impurities on the corrosion

behaviours and their effects on the corrosion mechanisms are necessary and urgent, which is required by establishing the mechanistic prediction models.

Mathematical prediction models

CO₂ and H₂S corrosion prediction models

The development of a mathematical corrosion prediction model based on physico-chemical processes is among the research hotspots in the fields of corrosion science and technology because it can assist engineers in foreseeing the corrosion issue and thus making decisions related to corrosion prevention and control issues [56]. There are three main types of mathematical prediction models [56,137]:

Mechanistic models: These models describe the mechanisms of the underlying reactions and have a strong theoretical background. Most of the constants appearing in this type of model have a clear physical meaning.

Semi-empirical models: These models are only partly based on firm theoretical hypotheses. Some of the constants appearing in these models have a clear physical meaning, while others are arbitrary best-fit parameters.

Empirical models: These models have very little or no theoretical background. Most constants used in them have no physical meaning.

Corrosion prediction is particularly important in the oil and gas industry, since the corrosion issue is highly connected with the safe operation of wells, pipelines and other facilities. CO₂ corrosion is the most common corrosion type in the oil and gas industry, and the earliest CO₂ corrosion model was published in 1975 by de Waard and Milliams [138], including only the CO₂ partial pressure and the temperature as the model input. It was then improved to kinds of CO₂ corrosion prediction models with more key parameters as the input variables, such as water chemistry, pH, scaling tendency, total pressure, fluid flow velocity, and hydraulic diameter. The famous CO₂ prediction models include the NORSOK model [139], the LIPUCOR model [140], the KSC model [141], the TULSA model [142], as listed in Table 4. The FREECORP [143,144] and MULTICORP [145] models are the most recently developed models, and the latter considers the complex effects of multiphase flow and product layers.

H₂S corrosion is another common corrosion problem in the oil and gas industry. A mechanistic prediction model was established for H₂S corrosion by Zheng et al. [97],

based on the hypothesis that there is a direct reduction of H₂S on the steel surface, as shown in Equation (41). Another mechanistic prediction model for CO₂/H₂S corrosion was also established by Zheng et al. [146–148] and is a useful reference when establishing supercritical CO₂ corrosion with H₂S and other impurities. It is also important in predicting liquid CO₂ corrosion, though there still remains a series of challenges to overcome.

Although there are many CO₂ corrosion prediction models, they can only be employed within the CO₂ partial pressure range of 0–2 MPa. When these models were applied to higher CO₂ partial pressure conditions, the predicted values were almost an order of magnitude higher than the experimental values [20,70]. The reason for this discrepancy should be attributed to the different corrosion characteristics under high-pressure conditions.

Mechanistic prediction model for corrosion in impure dense CO₂

Corrosion in dense CO₂ always occurs with a thin water layer with high ionic strength, and the dissolution behaviours of the impurity gases are non-ideal; thus, a new model should be generated for dense CO₂ conditions.

Currently, there is only one mechanistic model that specifically addresses the prediction of carbon steel corrosion in dense CO₂ phase with SO₂–O₂–H₂O impurities. A six-layer mechanistic model was established by Xiang et al. [19] by integrating the traditional CO₂ corrosion models [141,143,150–154] and the atmospheric corrosion model by Graedel [155]. The corrosion region was divided into six regions, namely, supercritical CO₂, interface, water film, deposition, electrodic, and solid (SIWDES), as shown in Figure 9. The effects of SO₂ and O₂ on the corrosion rate were considered, while the contribution of CO₂ to the corrosion rate was ignored. Only Equations (38) and (39) were considered as the cathodic reactions, and the mass transfer process was assumed to be diffusion controlled.

This model applied the following equation to calculate the diffusion rate of all components in the water and porous product scales for various components [19]:

$$\frac{\partial(\varepsilon c_j)}{\partial t} = -\frac{\partial}{\partial x} \left(\varepsilon^{1.5} D_j \frac{\partial c_j}{\partial x} \right) + \varepsilon R_j - \left(CR - \frac{\partial d_f}{\partial t} \right) \frac{\partial c_j}{\partial x} \quad (45)$$

The modified Three-Characteristic-Parameter Correlation (TCPC) model was introduced to modify the impact of the ionic strength on the activities of the species in the water film, allowing simple and accurate calculation of the ion

Table 4. Existing prediction models for corrosion in CO₂ environments [149].

Model	Developer (s)	Temperature (°C)		Pressure (bar) Max	CO ₂ partial pressure (bar)		pH	
		Min	Max		Min	Max	Min	Max
de Waard-Milliams	de Waard and Milliams	0	140	–	–	10	–	–
HYDROCOR	Shell	0	150	200	–	20	–	–
Cassandra 98	BP	–	–	–	–	10	–	–
NORSOK	Statoil, Saga, IFE	20	150	1000	–	10	3.5	6.5
CORMED	Elf	–	120	–	–	–	–	–
LIPUCOR	Total	20	150	250	–	50	–	–
KSC	IFE	5	150	250	–	50	–	–
TULSA	University of Tulsa	38	116	–	–	17	–	–
PREDICT	InterCorr International	20	200	–	–	100	2.5	7
SweetCor	Shell	5	121	–	0.2	170	–	–
Ohio	Ohio University	10	110	20	–	–	–	–

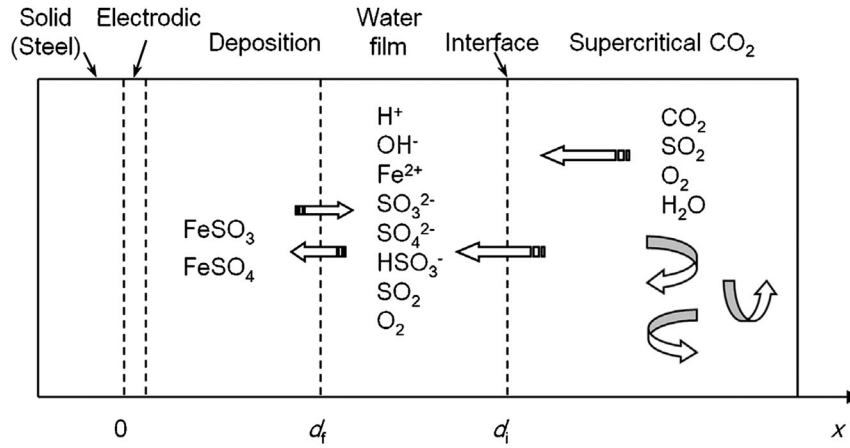


Figure 9. Schematic diagram of the SIWDES six-region model [19].

activity coefficients [156]:

$$\ln \gamma_{\pm} = -|z_+ z_-| A_{\phi} \left[\frac{I^{1/2}}{1 + b_1 I^{1/2}} + \frac{2}{b_1} \ln(1 + b_1 I^{1/2}) \right] + \frac{S_1}{T} \frac{I^{2n_1}}{v_+ + v_-} \quad (46)$$

The product film formation rate was calculated as follows [157]:

$$R_G = k_G \Delta c^{n_s} \quad (47)$$

For the hydrogen electrode current density i_{H^+} , the method proposed by Nordsveen et al. [150] was used. After the limit diffusion current density of oxygen was calculated, and according to current conservation, the anodic current density can be expressed as follows:

$$i_{Fe} = i_{H^+} + i_{O_2} \quad (48)$$

The relationship between the corrosion rate and the anode current density is as follows [158]:

$$CR = K_c \frac{i_{Fe} E W}{\rho} \quad (49)$$

A comparison of the corrosion rates predicted by this model and measured results is illustrated in Figure 10. The accuracy of this model seems to be high, especially for cases with high SO_2 concentration and RH. However, for cases with extremely low SO_2 concentration, the accuracy of this model seems to be low. These results suggested that the effect of dissolved CO_2 should be considered for conditions with low SO_2 concentrations. For low-RH conditions, the results of this model were also not satisfactory.

Notwithstanding, this model only included the influence of SO_2 , O_2 , and H_2O , while the impact of the other possible impurities (such as NO_x and H_2S) was not addressed. This model was also based on several assumptions, including the RDS and the cathodic processes of the corrosion. The corrosion product layer growth model was based on the $FeCO_3$ layer growth model, which might be questionable. There seems to be a need to develop a more reliable mechanistic prediction model for steel corrosion in dense CO_2 with multiple impurities. This task will not be easy, as researchers must find accurate mathematical descriptions for the physical and chemical processes in several different layers, which will

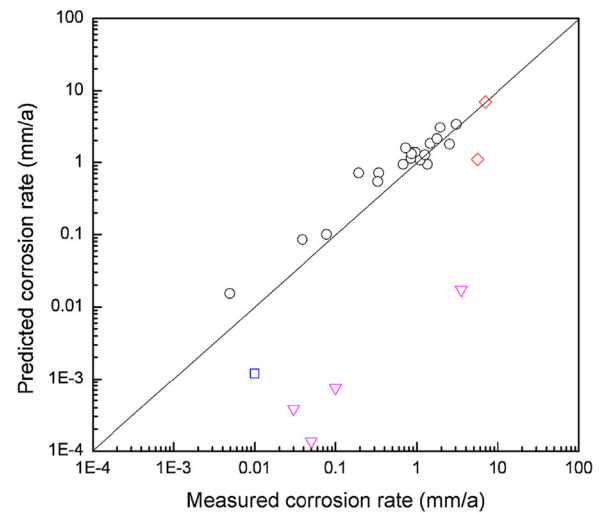


Figure 10. Comparison between measured corrosion rates and predicted corrosion rates [19] (□ Dugstad et al. [27]; ◇ Choi et al. [23]; ○ Xiang et al. [15,43,45,46]; ▽ Farelas et al. [88]).

strongly rely on experimental mechanistic studies of the dense CO_2 corrosion.

Knowledge gaps for mechanistic model of corrosion in impure dense CO_2

The following challenges still remain for establishing the mechanistic prediction model for general corrosion in impure dense CO_2 environments:

- (i) The bulk phase reaction mechanisms and kinetics with multiple impurities;
- (ii) The phase equilibrium model considering all the possible impurities, to determine the amount of dissolved impurities in the condensed phase;
- (iii) The water condensation mechanisms and kinetics, to determine the water layer thickness and water chemistry;
- (iv) The ionisation equilibrium model of the dissolved species;
- (v) The constitution of the anodic and cathodic reactions and their corresponding kinetics;
- (vi) The formation mechanisms and kinetics of the product layers and their corresponding properties;

- (vii) The mass transfer models in the dynamic bulk CO₂, aqueous phase and product layers.

Notably, all of the above discussion addresses general corrosion prediction, while the prediction of localised corrosion in both dense CO₂ and low partial pressure CO₂ is a huge challenge. Apart from the mechanistic models, semi-empirical and empirical models may be better choices until almost all the above fundamental questions are correctly solved. The neural network model created by Sim et al. [21] through applying the potentiodynamic polarisation data from the corrosion tests also seems to be a good approach.

Corrosion control strategies

Generally, if water is not thoroughly removed from the impure CO₂ streams, using CRAs, coatings, and inhibitors are the usual corrosion control measures for CCS CO₂ pipelines. Usually, the compact layer of FeCO₃ can have a favourable protection to the substrate metal, and Sim et al. [6] noted it as a potential source of corrosion protection for CO₂ transportation; however, the presence of acidic gases will definitely weaken the protectiveness of FeCO₃ layer, since it can be dissolved by the stronger acids. Stainless steels usually show excellent corrosion resistance, but due to their high costs, they are unlikely to be the best option for CO₂ pipeline transportation in a large scale. Barker et al. [67] pointed out that it is unlikely that CRAs will offer any significant benefit in terms of mitigating corrosion as the protective passive film will not be stable under the conditions in the aqueous phase due to the low pH.

The detailed material selection issue for supercritical CO₂ transport can be referred to the work by Paul et al. [159–161]. Appropriate steels suitable for CO₂ transportation for the CCS purposes need to be developed and selected based on laboratory testing and the evaluation of the application limits [33]. The other two corrosion control methods are discussed as follows:

Coatings

Coatings are thought to be among the most important corrosion control strategies. Morks et al. [50] indicated that the inhibition efficiency of Mn–Mg–Zn phosphate coatings was low when the pH was low. One of the coatings was selected by Zhang et al. [52] as a good candidate for internal coatings of the CO₂ pipeline when testing the performance of three polymer coatings in CO₂ containing impurities and possible solutions.

Recently, Paul [51] reported the use of a thermal spray CRA coating to mitigate the corrosion of carbon steel in an environment containing supercritical CO₂, H₂S, and an aqueous phase. Thermally sprayed CRA coatings were proposed as a cost-effective corrosion mitigation method for infrastructure that is likely to be in contact with wet supercritical CO₂ containing H₂S. However, they also stated that care must be taken to ensure that the thermally sprayed layer does not have any through porosity. Otherwise, such coatings with through porosity may accelerate corrosion of the underlying steel due to galvanic interactions.

However, Sim et al. [6] argued that internal pipeline coatings such as polymeric coatings are not feasible as anti-corrosion technology for long-distance dense CO₂

transportation, due to the high operating pressure and potentially accelerating corrosion in the presence of likely defects. It seems that such coating is not appropriate for CO₂ pipeline corrosion control.

Inhibitors

If dehydration is not applied to the CO₂ purification process, inhibitors can be selected to control the internal corrosion of the CO₂ pipeline, which is similar to the internal corrosion control strategy in oil and gas pipelines. Taking natural gas transportation as an example, wet gas transportation is usually adopted rather than dry gas transportation, even for some gas fields with high H₂S concentrations (e.g. Puguang Gas field in China and East Crossfield in Canada), due to the lower operational cost for wet gas transportation.

The performance of various inhibitors in CO₂-saturated aqueous phase has been studied for the oil and gas transportation purpose [3,162–171], and most of the tests were under low CO₂ partial pressure conditions. Imidazoline-based inhibitors are extensively used in oil and gas industry to mitigate CO₂ corrosion. When they are used in supercritical CO₂ phase, the performance of these inhibitors remains questionable and must be further verified. Therefore, corrosion inhibition practices employed in oil and gas fields must be carefully applied to CCS [6].

The performance of several inhibitors in a supercritical CO₂-saturated water environment was tested by Zhang et al. [49]; however, the performance of inhibitors in a water-saturated supercritical CO₂ environment has seldom been addressed. Morks et al. [50] tried a vanadate inhibitor for CCS CO₂ transportation, but the inhibition efficiency was almost nil when the pH was between 1 and 3, even in combination with Mn–Mg–zinc phosphate coating.

The challenge of using inhibitors in dense CO₂ is that it is hard to find an inhibitor to reduce the corrosion rate of steel in the presence of a number of acidic gas impurities, which can always induce extremely low pH in the condensates. The diffusion ability of an inhibitor in dense CO₂ is another issue to be considered. For CCS purpose, CO₂-soluble inhibitors or high diffusion rate of corrosion inhibitors in CO₂ is required [6]. They also have to be the water-soluble inhibitors, for they will eventually dissolve in the water film on the steel surface to inhibit corrosion in dense CO₂ phase.

Neutralising amines (pH stabilisation) is a potential option to mitigate corrosion caused by strong acids in systems where water condenses onto a steel surface, and choosing a proper amine always requires considering a number of properties, including boiling point, the effect of excess amine, the vapour–liquid equilibrium, the base strength and potential salt formation [67]. This technique can be rarely used with formation water systems for it has the drawback of leading to excessive scaling. The side effects of the chemicals used to inhibit corrosion on the environment must be also considered when selecting the chemicals.

It is still difficult to choose the best way to control the corrosion problems of impure CO₂ pipelines, though most of the existing CO₂ projects choose controlling the water content as solving method, while they always transport CO₂ from the natural sources with less acidic gas impurities rather than the anthropogenic CO₂.

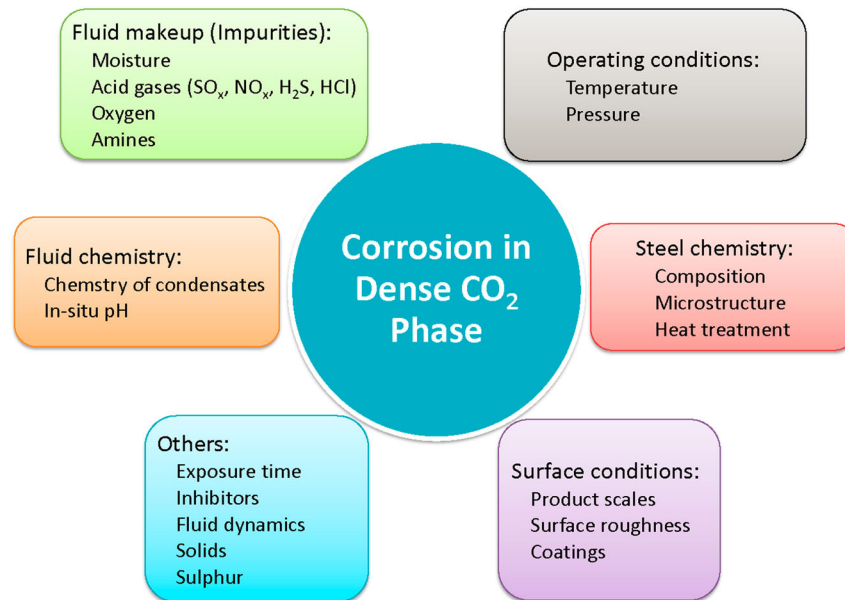


Figure 11. Summaries of the influential parameters of steel corrosion in dense CO₂ environments.

Research prospects

The summarised influential parameters of supercritical CO₂ corrosion are illustrated in Figure 11. Overall, studies related to the corrosion of pipeline steel in dense CO₂ transportation systems remain relatively limited, and more investigations are required to improve the understanding of corrosion mechanisms. A number of influential parameters with great impact on the corrosion process require further and deeper studies. The urgent topics to be investigated include the following:

- (i) The impact of flow dynamics, amines, sulphur, and solids. The flow dynamics have a significant influence on the mass transfer process and product scales. Solids may not exist in the CO₂ pipeline, but the corrosion product scales falling off from the inner wall of the pipeline by the mechanical force might act as solids, and their corrosion-erosion effect should be considered. The influence of possible hydrates on the corrosion also requires further evaluation. The impact of the amines and their degradation products, such as formate and acetate, needs to be reconsidered in supercritical CO₂ systems. The influence of sulphur on corrosion in the supercritical CO₂ environment also needs to be evaluated. The impact of H₂O and O₂ on the corrosion rate should be re-evaluated, since there are opposite conclusions in the open literature.
- (ii) More online research methods are also desirable to investigate the intermediate steps of the corrosion process. Using electrochemical techniques in the dense CO₂ phase, aqueous phase, and under ambient pressure conditions might be valuable and useful for the investigation of mechanisms, especially for the cathodic processes. The composition of product scales under multiple acidic gas impurity conditions and the mechanical property studies of corrosion product scales. *In situ* observation tools can be applied to observe the evolution process of product scales, to obtain the real surface morphology excluding the influence of environmental change (when bringing the specimens from a high-pressure to a normal-pressure environment).
- (iii) The synergistic corrosion mechanism of steel under supercritical CO₂ with multiple acidic gas impurities (SO₂, NO_x, H₂S, and HCl). The synergistic corrosion mechanism is complicated by these acidic gases and needs systematic investigation. The cathodic process of the corrosion is not clear, especially for conditions with various impurities. The cross chemical reaction mechanisms of impurities also need to be examined. These are all crucial for establishing a mechanistic prediction model with high accuracy. Localised corrosion, HIC and SCC mechanisms of CO₂ pipeline steel and the prevention methods and corresponding standards under supercritical CO₂ environments also need to be addressed and formulated.
- (iv) The establishment of mechanistic prediction model for steel corrosion in dense CO₂ phase with various acidic gas impurities. There are many CO₂ corrosion prediction models, but they are not accurate for predicting corrosion in dense CO₂ phase with thin water films. The defects of the SIWDES model should be overcome, including the consideration of more impurities, dissolution, and ionisation equilibrium models, anodic and cathodic reaction mechanisms and kinetics, a mass transfer model and the kinetics of the product layer formation, etc. The setting up of mathematical mechanistic model for uniform corrosion prediction that can reflect the effects of the primary variables with high accuracy is challenging in dense CO₂ environment with various impurities.
- (v) Research on anti-corrosion measures for CO₂ pipeline transportation with multiple acidic gas impurities: inhibitors and new CRAs are needed for the transportation of CO₂ with multiple acidic gas impurities. The inhibitors with high corrosion inhibition efficiency in the dense CO₂ phase are needed, including the selecting of the existing inhibitors or the synthesis of new inhibitors. The diffusion behaviours of potential inhibitor candidates in the dense CO₂ phase need to be addressed.

Using the existing CRAs seems to be not economically feasible, and there is an urgent need for developing the new CRAs with low cost and excellent corrosion resistance under low pH condition for CCS. The role of alloying elements needs to be determined to find the optimised steel compositions to satisfy the corrosion resistance, strength, properties, and weldability targets required for the transportation of dense CO₂ with various acidic gas impurities.

Conclusions

Steel corrosion in dense CO₂ phase is affected by various factors, including physical, environmental, and metallurgical variables. Based on the experimental results in the open literature, this paper systematically analyses the influential parameters and their impact mechanisms on pipeline steel corrosion in dense CO₂ phase with impurities. The mathematical models are also reviewed and highlighted. Several conclusions can be drawn:

- (i) The effects of impurities, pressure, temperature, flow, exposure time, product layers, and steel chemistry are reviewed. Neglected influential parameters by the current researchers have been highlighted, including the impact of flow dynamics as well as various amines, sulphur, and solids. Further research prospects for pipeline steel corrosion in dense CO₂ phase with multiple acidic gas impurities are also suggested to further understand the corrosion mechanisms and establish mechanistic corrosion prediction models, such as synergistic corrosion mechanisms, compositions and properties of product layers, and corrosion control strategies.
- (ii) The knowledge gaps regarding a dense CO₂ corrosion prediction model include bulk phase reaction mechanisms, a phase equilibrium model for impurities, water condensation mechanisms and kinetics, anodic and cathodic reaction mechanisms and kinetics, kinetics of product layer formation, and mass transfer models.
- (iii) New CRAs with high corrosion resistance and inhibitors with high inhibition efficiency are needed for the transportation of CO₂ with multiple acidic gas impurities, though it seems to be difficult to find an effective inhibitor that works well under dense CO₂ and low pH conditions. pH stabilisation is a potential option to mitigate corrosion caused by strong acidic gases in dense CO₂.
- (iv) It is still difficult to select the best ways to control corrosion in dense CO₂ transportation for large scale CCS among options such as controlling the water content, eliminating acidic gas impurities, employing inhibitors and coatings, and using CRAs. The understanding, prediction, and control strategies for supercritical CO₂ corrosion still remain key challenges in meeting the safety requirements of CO₂ transportation for CCS purpose at a large scale.

Disclosure statement

No potential conflict of interest was reported by the authors.

Funding

This work was financially supported by National Natural Science Foundation of China (Grant No. 51604289), Beijing Natural Science Foundation (Grant No. 2172048), Science Foundation of China University of Petroleum, Beijing (Grant Nos. 2462014YJRC043 and 2462015YQ0402), and Open Foundation of China State Key Lab of Power Systems (Grant No. SKLD16KZ10).

References

- [1] de Visser E, Hendriks C, Barrio M, et al. Dynamis CO₂ quality recommendations. *Int J Greenh Gas Con.* 2008;2(4):478–484.
- [2] Johnson K, Holt H, Helle K, et al. Mapping of potential HSE issues related to large-scale capture, transport and storage of CO₂. Det Norsk Veritas, Horvik, Norway; 2008.
- [3] Zheng L, Landon J, Koebecke NC, et al. Suitability and stability of 2-mercaptobenzimidazole as a corrosion inhibitor in a post-combustion CO₂ capture system. *Corrosion.* 2015;71(6):692–702.
- [4] Xiang Y, Yan M, Choi Y-S, et al. Time-dependent electrochemical behavior of carbon steel in MEA-based CO₂ capture process. *Int J Greenh Gas Con.* 2014;30:125–132.
- [5] Xiang Y, Choi Y-S, Yang Y, et al. Corrosion of carbon steel in MDEA-based CO₂ capture plants under regenerator conditions: effects of O₂ and heat-stable salts. *Corrosion.* 2015;71(1):30–37.
- [6] Sim S, Cole IS, Choi YS, et al. A review of the protection strategies against internal corrosion for the safe transport of supercritical CO₂ via steel pipelines for CCS purposes. *Int J Greenh Gas Con.* 2014;29:185–199.
- [7] Cole IS, Corrigan P, Sim S, et al. Corrosion of pipelines used for CO₂ transport in CCS: is it a real problem? *Int J Greenh Gas Con.* 2011;5(4):749–756.
- [8] Pfennig A, Zastrow P, Kranzmann A. Influence of heat treatment on the corrosion behaviour of stainless steels during CO₂-sequestration into saline aquifer. *Int J Greenh Gas Con.* 2013;15:213–224.
- [9] Choi YS, Duan D, Nescic S, et al. Effect of oxygen and heat stable salts on the corrosion of carbon steel in MDEA-based CO₂ capture process. *Corrosion.* 2010;66(12):125004.
- [10] Schremp FW, Roberson GR. Effect of supercritical carbon dioxide (CO₂) on construction materials. *SPE J.* 1975;15(3):227–233.
- [11] DeBerry DW, Clark WS. Corrosion due to use of carbon dioxide for enhanced oil recovery. Austin (TX): DOE; 1979.
- [12] Propp WA, Carleson TE, Wai CM, et al. Corrosion in supercritical fluids. Idaho Falls: Idaho National Engineering Laboratory; 1996.
- [13] Hua Y, Barker R, Charpentier T, et al. Relating iron carbonate morphology to corrosion characteristics for water-saturated supercritical CO₂ systems. *J Supercrit Fluids.* 2015;98:183–193.
- [14] Zhang Y, Pang X, Qu S, et al. The relationship between fracture toughness of CO₂ corrosion scale and corrosion rate of X65 pipeline steel under supercritical CO₂ condition. *Int J Greenh Gas Con.* 2011;5(6):1643–1650.
- [15] Xiang Y, Wang Z, Li Z, et al. Effect of exposure time on the corrosion rates of X70 Steel in supercritical CO₂/SO₂/O₂/H₂O environments. *Corrosion.* 2013;69(3):251–258.
- [16] Sun C, Sun J, Wang Y, et al. Synergistic effect of O₂, H₂S and SO₂ impurities on the corrosion behavior of X65 steel in water-saturated supercritical CO₂ system. *Corros Sci.* 2016;107:193–203.
- [17] Yevtushenko O, Bettge D, Bäßler R, et al. Corrosion of CO₂ transport and injection pipeline steels due to the condensation effects caused by SO₂ and NO₂ impurities. *Mater Corros.* 2015;66(4):334–341.
- [18] Zhang Y, Pang X, Qu S, et al. Discussion of the CO₂ corrosion mechanism between low partial pressure and supercritical condition. *Corros Sci.* 2012;59:186–197.
- [19] Xiang Y, Wang Z, Xu M, et al. A mechanistic model for pipeline steel corrosion in supercritical CO₂-SO₂-O₂-H₂O environments. *J Supercrit Fluids.* 2013;82:1–12.
- [20] Zhang Y, Gao K, Schmitt G, et al. Modeling steel corrosion under supercritical CO₂ conditions. *Mater Corros.* 2013;64(6):478–485.
- [21] Sim S, Cavanaugh MK, Corrigan P, et al. Aqueous corrosion testing and neural network modeling to simulate corrosion of supercritical CO₂ pipelines in the carbon capture and storage cycle. *Corrosion.* 2012;69(5):477–486.

- [22] Ayello F, Sridhar N, Evans K, et al. Effect of liquid impurities on corrosion of carbon steel in supercritical CO₂. Proceedings of the 8th International Pipeline Conference (IPC2010), September 27–October 1, Calgary, Alberta, Canada; 2010.
- [23] Choi YS, Nestic S, Young D. Effect of impurities on the corrosion behavior of CO₂ transmission pipeline steel in supercritical CO₂-water environments. *Environ Sci Technol*. 2010;44(23):9233–9238.
- [24] Choi Y-S, Hassani S, Vu TN, et al. Effect of H₂S on the corrosion behavior of pipeline steels in supercritical and liquid CO₂ environments. CORROSION/2015, NACE International, Dallas, TX, USA, Paper No. 5927, 2015.
- [25] Choi Y-S, Nestic S. Determining the corrosive potential of CO₂ transport pipeline in high pCO₂-water environments. *Int J Greenh Gas Con*. 2011;5(4):788–797.
- [26] Collier J, Shi C, Papavinasam S, et al. Effect of impurities on the corrosion performance of steels in supercritical carbon dioxide: optimization of experimental procedure. CORROSION/2013, NACE International, Orlando, FL, USA, 2013.
- [27] Dugstad A, Morland B, Clausen S. Corrosion of transport pipelines for CO₂-effect of water ingress. *Energy Proc*. 2011;4:3063–3070.
- [28] Hua Y, Barker R, Neville A. Effect of temperature on the critical water content for general and localised corrosion of X65 carbon steel in the transport of supercritical CO₂. *Int J Greenh Gas Con*. 2014;31:48–60.
- [29] Hua Y, Barker R, Neville A. Comparison of corrosion behaviour for X-65 carbon steel in supercritical CO₂-saturated water and water-saturated/unsaturated supercritical CO₂. *J Supercrit Fluids*. 2015;97:224–237.
- [30] Hua Y, Barker R, Neville A. The influence of SO₂ on the tolerable water content to avoid pipeline corrosion during the transportation of supercritical CO₂. *Int J Greenh Gas Con*. 2015;37:412–423.
- [31] Hua Y, Barker R, Neville A. The effect of O₂ content on the corrosion behaviour of X65 and 5Cr in water-containing supercritical CO₂ environments. *Appl Surf Sci*. 2015;356:499–511.
- [32] Hua Y, Barker R, Neville A. Understanding the influence of SO₂ and O₂ on the corrosion of carbon steel in water-saturated supercritical CO₂. *Corrosion*. 2015;71(5):667–683.
- [33] Jacobson GA. Pipeline corrosion issues related to carbon capture, transportation, and storage. *Mater Perform*. 2013;53:24–31.
- [34] Jiang X, Qu D, Song X, et al. Impact of water content on corrosion behavior of CO₂ transportation pipeline. CORROSION/2015, NACE International, Dallas, TX, USA, Paper No. 5844, 2015.
- [35] McGrail BP, Schaeff HT, Glezakou VA, et al. Water reactivity in the liquid and supercritical CO₂ phase: has half the story been neglected? *Energy Procedia*. 2009;1:3415–3419.
- [36] Ruhl AS, Kranzmann A. Corrosion behavior of various steels in a continuous flow of carbon dioxide containing impurities. *Int J Greenh Gas Con*. 2012;9(0):85–90.
- [37] Ruhl AS, Kranzmann A. Corrosion in supercritical CO₂ by diffusion of flue gas acids and water. *J Supercrit Fluids*. 2012;68:81–86.
- [38] Ruhl AS, Kranzmann A. Investigation of corrosive effects of sulphur dioxide, oxygen and water vapour on pipeline steels. *Int J Greenh Gas Con*. 2013;13:9–16.
- [39] Sim S, Bocher F, Cole IS, et al. Investigating the effect of water content in supercritical CO₂ as relevant to the corrosion of carbon capture and storage pipelines. *Corrosion*. 2014;70(2):185–195.
- [40] Sim S, Cole IS, Bocher F, et al. Investigating the effect of salt and acid impurities in supercritical CO₂ as relevant to the corrosion of carbon capture and storage pipelines. *Int J Greenh Gas Con*. 2013;17:534–541.
- [41] Sun J, Sun C, Zhang G, et al. Effect of O₂ and H₂S impurities on the corrosion behavior of X65 steel in water-saturated supercritical CO₂ system. *Corros Sci*. 2016;107:31–40.
- [42] Wei L, Pang X, Gao K. Effect of small amount of H₂S on the corrosion behavior of carbon steel in the dynamic supercritical CO₂ environments. *Corros Sci*. 2016;103:132–144.
- [43] Xiang Y, Wang Z, Li Z, et al. Effect of temperature on the corrosion behavior of X70 steel in high pressure CO₂/SO₂/O₂/H₂O environments. *Corros Eng Sci Technol*. 2013;48(2):121–129.
- [44] Xiang Y, Wang Z, Li Z, et al. Long term corrosion of X70 steel and iron in humid supercritical CO₂ with SO₂ and O₂ impurities. *Corros Eng Sci Technol*. 2013;48(5):395–398.
- [45] Y. Xiang, Z. Wang, C. Xu, C. Zhou, Z. Li, and W. Ni: 'Impact of SO₂ concentration on the corrosion rate of X70 steel and iron in water-saturated supercritical CO₂ mixed with SO₂', *J Supercrit Fluids*. 2011;58(2): 286–294.
- [46] Xiang Y, Wang Z, Yang X, et al. The upper limit for moisture content in CO₂ pipeline transport. *J Supercrit Fluids*. 2012;67:14–21.
- [47] Xu M, Zhang Q, Yang X, et al. Impact of surface roughness and humidity on X70 steel corrosion in supercritical CO₂ mixture with SO₂, H₂O, and O₂. *J Supercrit Fluids*. 2016;107:286–297.
- [48] Zhang Y, Gao K, Schmitt G. Water effect on steel under supercritical CO₂ condition. CORROSION/2011, NACE International, Houston, TX, USA, Paper No. 11378, 2011.
- [49] Zhang Y, Gao K, Schmitt G. Inhibition of steel corrosion under aqueous supercritical CO₂ conditions. CORROSION/2011, NACE International, Houston, TX, USA, Paper No. 11379, 2011.
- [50] Morks MF, Corrigan PA, Cole IS. Mn–Mg based zinc phosphate and vanadate for corrosion inhibition of steel pipelines transport of CO₂ rich fluids. *Int J Greenh Gas Con*. 2012;7:218–224.
- [51] Paul S. Thermally sprayed corrosion resistant alloy coatings on carbon steel for use in supercritical CO₂ environments. CORROSION/2015, NACE International, Dallas, TX, USA, Paper No. 5939, 2015.
- [52] Zhang X, Zevenbergen JF, Spruijt MPN, et al. Corrosion of pipe steel in CO₂ containing impurities and possible solutions. *Energy Proc*. 2013;37:3147–3159.
- [53] Rouillard F, Charton F, Moine G. Corrosion behavior of different metallic materials in supercritical CO₂ at 550°C and 250 bars. CORROSION/2010, NACE International, San Antonio, TX, USA, Paper No. 10195, 2010.
- [54] Moore R, Conboy T. Metal corrosion in a supercritical carbon dioxide-liquid sodium power cycle. Albuquerque: Sandia National Laboratories; 2012.
- [55] Kermani MB, Morshed A. Carbon dioxide corrosion in oil and gas production – a compendium. *Corrosion*. 2003;59(8):659–683.
- [56] Nestic S. Key issues related to modelling of internal corrosion of oil and gas pipelines – a review. *Corros Sci*. 2007;49(12):4308–4338.
- [57] Gibbs JP. Corrosion of various engineering alloys in supercritical carbon dioxide. Massachusetts Institute of Technology, 2010.
- [58] Firouzdor V, Sridharan K, Cao G, et al. Corrosion of a stainless steel and nickel-based alloys in high temperature supercritical carbon dioxide environment. *Corros Sci*. 2013;69:281–291.
- [59] Oosterkamp A, Ramsen J. State-of-the-art overview of CO₂ pipeline transport with relevance to offshore pipelines. POL-O-2007-138-A, POLYTEC, 2008.
- [60] Jiang X, Qu D, Liu X. Supercritical CO₂ pipeline transportation and safety. *Oil Gas Storage Transp*. 2013;32(8):809–813.
- [61] Zhao X. Overview of CCUS corrosion control technologies and discussion on the problems. 2nd Corrosion and Protection Technologies of Petroleum and Petrochemistry Conference of China, Pengshan, China; 2016.
- [62] Brown J, Graver B, Gulbrandsen E, et al. Update of DNV recommended practice RP-J202 with focus on CO₂ corrosion with impurities. *Energy Proc*. 2014;63:2432–2441.
- [63] Dugstad A, Halseid M, Morland B. Effect of SO₂ and NO₂ on corrosion and solid formation in dense phase CO₂ pipelines. *Energy Proc*. 2013;37:2877–2887.
- [64] Dugstad A, Halseid M, Morland B. Testing of CO₂ specifications with respect to corrosion and bulk phase reactions. *Energy Proc*. 2014;63:2547–2556.
- [65] Dugstad A, Halseid M, Morland B, et al. Corrosion in dense phase CO₂ – the impact of depressurisation and accumulation of impurities. *Energy Proc*. 2013;37:3057–3067.
- [66] Wei L, Zhang Y, Pang X, et al. Corrosion behaviors of steels under supercritical CO₂ conditions. *Corros Rev*. 2015;33(3–4):151–174.
- [67] Barker R, Hua Y, Neville A. Internal corrosion of carbon steel pipelines for dense-phase CO₂ transport in carbon capture and storage (CCS) – a review. *Int Mater Rev*. 2016: 1–31.
- [68] Sarrade S, Féron D, Rouillard F, et al. Overview on corrosion in supercritical fluids. *J Supercrit Fluids*. 2016. Accepted.

- [69] West JM. Design and operation of a supercritical CO₂ pipeline-compression system SACROC Unit, Scurry County, TX. SPE/1974, Houston, TX, 1974, SPE International, Paper No. 4804.
- [70] Kongshaug KO, Seiersten M. Baseline experiments for the modeling of corrosion at high CO₂ pressure. CORROSION/2004, NACE International New Orleans, LA, Paper No. 04630, 2004.
- [71] Abbas Z, Mezher T, Abu-Zahra MRM. CO₂ purification. Part II: techno-economic evaluation of oxygen and water deep removal processes. *Int J Greenh Gas Con.* 2013;16:335–341.
- [72] Song KY, Kobayashi R. Water content of CO₂ in equilibrium with liquid water and/or hydrates. *SPE Form Eval.* 1987;2(4):500–508.
- [73] King MB, Mubarak A, Kim JD, et al. The mutual solubilities of water with supercritical and liquid carbon dioxide. *J Supercrit Fluids.* 1992;5(4):296–302.
- [74] Munkejord ST, Jakobsen JP, Austegard A, et al. Thermo- and fluid-dynamical modelling of two-phase multi-component carbon dioxide mixtures. *Int J Greenh Gas Con.* 2010;4(4):589–596.
- [75] Spycher N, Pruess K, Ennis-King J. CO₂-H₂O mixtures in the geological sequestration of CO₂. I. Assessment and calculation of mutual solubilities from 12 to 100 degrees C and up to 600 bar. *Geochim Cosmochim Acta.* 2003;67(16):3015–3031.
- [76] Song KY, Kobayashi R. The water content of a CO₂-rich gas mixture containing 5.31 mol% methane along the three-phase and supercritical conditions. *J Chem Eng Data.* 1990;35(3):320–322.
- [77] Foltran S, Vosper ME, Suleiman NB, et al. Understanding the solubility of water in carbon capture and storage mixtures: an FTIR spectroscopic study of H₂O+CO₂+N₂ ternary mixtures. *Int J Greenh Gas Con.* 2015;35:131–137.
- [78] Cole IS, Paterson DA, Corrigan P, et al. State of the aqueous phase in liquid and supercritical CO₂ as relevant to CCS pipelines. *Int J Greenh Gas Con.* 2012;7:82–88.
- [79] Yevtushenko O, Bäßler R. Water impact on corrosion resistance of pipeline steels in circulating supercritical CO₂ with SO₂- and NO₂- impurities. CORROSION/2014, NACE International, San Antonio, TX, USA, Paper No. 3838, 2014.
- [80] Thodla R, Francois A, Sridhar N. Materials performance in supercritical CO₂ environments. CORROSION/2009, Atlanta, GA, 03/22/2009, 2009, NACE International.
- [81] Vernon WHJ. A laboratory study of the atmospheric corrosion of metals. Part II. Iron: the primary oxide film. Part III. The secondary product or rust (Influence of sulphur dioxide, carbon dioxide, and suspended particles on the rusting of iron). *Trans Faraday Soc.* 1935;31(2):1668–1699.
- [82] Li X, Dong C, Xiao K, et al. The initial corrosion behavior and mechanism of metal in atmosphere (in Chinese). Beijing: Science Press; 2009.
- [83] Zhong X, Zhang G, Qiu Y, et al. The corrosion of tin under thin electrolyte layers containing chloride. *Corros Sci.* 2013;66:14–25.
- [84] Zhong X, Zhang G, Qiu Y, et al. In situ study the dependence of electrochemical migration of tin on chloride. *Electrochem Commun.* 2013;27:63–68.
- [85] Beck J, Lvov S, Fedkin M, et al. Electrochemical system to study corrosion of metals in supercritical CO₂ fluids. CORROSION/2011, Houston, TX, USA. Paper No. 11380, 2011, NACE International.
- [86] Tang Y, Guo XP, Zhang GA. Corrosion behaviour of X65 carbon steel in supercritical-CO₂ containing H₂O and O₂ in carbon capture and storage (CCS) technology. *Corros Sci.* 2017. DOI:10.1016/j.corsci.2017.01.028.
- [87] Jolly WL. Modern inorganic chemistry. New York (NY): McGraw-Hill, Inc; 1991.
- [88] Farelas F, Choi YS, Nešić S. Corrosion behavior of API 5L X65 carbon steel under supercritical and liquid CO₂ phases in the presence of H₂O and SO₂. *Corrosion.* 2012;69(3):243–250.
- [89] Dugstad A, Halseid M, Morland B. Experimental techniques used for corrosion testing in dense phase CO₂ with flue gas impurities. CORROSION/2014, San Antonio, TX, USA. Paper No. 4383, 2014.
- [90] Paschke B, Kather A. Corrosion of pipeline and compressor materials due to impurities in separated CO₂ from fossil-fuelled power plants. *Energy Proc.* 2012;23:207–215.
- [91] Sun C, Wang Y, Sun J, et al. Effect of impurity on the corrosion behavior of X65 steel in water-saturated supercritical CO₂ system. *J Supercrit Fluids.* 2016;116:70–82.
- [92] Halseid M, Dugstad A, Morland B. Corrosion and bulk phase reactions in CO₂ transport pipelines with impurities: review of recent published studies. *Energy Proc.* 2014;63:2557–2569.
- [93] Kolman DG, Ford DK, Butt DP, et al. Corrosion of 304 stainless steel exposed to nitric acid-chloride environments. *Corrosion Sci.* 1997;39(12):2067–2093.
- [94] Osarolube E, Owate IO, Oforka NC. Corrosion behaviour of mild and high carbon steels in various acidic media. *Sci Res Essays.* 2008;3(6):224–228.
- [95] Barbosa MA. The pitting resistance of AISI 316 stainless steel passivated in diluted nitric acid. *Corros Sci.* 1983;23(12):1293–1305.
- [96] Sandana D, Dale M, Charles EA, et al. Transport of gaseous and dense carbon dioxide in pipelines: is there an internal stress corrosion cracking risk? CORROSION/2013, Orlando, FL, USA, 2013, NACE International, Paper No. 2516.
- [97] Zheng Y, Brown B, Nešić S. Electrochemical study and modeling of H₂S corrosion of mild steel. *Corrosion.* 2014;70(4):351–365.
- [98] Zhang GA, Zeng Y, Guo XP, et al. Electrochemical corrosion behavior of carbon steel under dynamic high pressure H₂S/CO₂ environment. *Corros Sci.* 2012;65:37–47.
- [99] Ning J, Zheng Y, Brown B, et al. A thermodynamic model for the prediction of mild steel corrosion products in an aqueous hydrogen sulfide environment. *Corrosion.* 2015;71(8):945–960.
- [100] Ning J, Zheng Y, Young D, et al. Thermodynamic study of hydrogen sulfide corrosion of mild steel. *Corrosion.* 2014;70(4):375–389.
- [101] Pessu F, Barker R, Neville A. Early stages of pitting corrosion of UNS K03014 carbon steel in sour corrosion environments: the influence of CO₂, H₂S and temperature. CORROSION/2015, Dallas, TX, USA, 2015, NACE International.
- [102] Wei L, Pang X, Gao K. Corrosion of low alloy steel and stainless steel in supercritical CO₂/H₂O/H₂S systems. *Corros Sci.* 2016.
- [103] Zeng Y, Pang X, Shi C, et al. Influence of impurities on corrosion performance of pipeline steels in supercritical carbon dioxide. CORROSION/2015, NACE International, Dallas, TX, USA, Paper No. 5755, 2015.
- [104] Ayello F, Evans K, Thodla R, et al. Effect of impurities on corrosion of steel in supercritical CO₂. CORROSION/2010, Houston, TX, USA, 2010, NACE International, Paper No. 10193.
- [105] Xu M, Zhang Q, Wang Z, et al. Effect of high-concentration O₂ on corrosion behavior of X70 steel in water-containing supercritical CO₂ with SO₂. *Corrosion.* 2017;73(3):290–302.
- [106] Rosli NR, Choi Y-S, Young D. Impact of oxygen ingress in CO₂ corrosion of mild steel. CORROSION/2014, San Antonio, TX, USA, 2014, NACE International, Paper No. 4299.
- [107] Allam IM, Arlow JS, Saricimen H. Initial stages of atmospheric corrosion of steel in the Arabian Gulf. *Corros Sci.* 1991;32(4):417–432.
- [108] Yamashita M, Miyuki H, Matsuda Y, et al. The long term growth of the protective rust layer formed on weathering steel by atmospheric corrosion during a quarter of a century. *Corros Sci.* 1994;36(2):283–299.
- [109] Nishimura R, Shiraiishi D, Maeda Y. Hydrogen permeation and corrosion behavior of high strength steel MCM 430 in cyclic wet-dry SO₂ environment. *Corros Sci.* 2004;46(1):225–243.
- [110] Schmitt G. Fundamental aspects of CO₂ corrosion. In: Hausler RH, editor. *Advances in CO₂ corrosion.* Houston (TX): NACE; 1984. p. 10.
- [111] Gao X, Brown B, Nestic S. Effect of chloride on localized corrosion initiation of carbon steel in a CO₂ aqueous environment. CORROSION/2014, San Antonio, TX, USA, 2014, NACE International, Paper No. 3880.
- [112] Chen C. Research on electrochemical behavior and corrosion scale characteristics of CO₂ corrosion for tubing and casing steel [PhD thesis]. Xi'an: Northwestern Polytechnical University; 2002.
- [113] Xu M, Li W, Zhou Y, et al. Effect of pressure on corrosion behavior of X60, X65, X70, and X80 carbon steels in water-unsaturated supercritical CO₂ environments. *Int J Greenh Gas Con.* 2016;51:357–368.
- [114] Shadley JR, Shirazi SA, Dayalan E, et al. CO₂ corrosion prediction in pipe flow under FeCO₃ scale forming conditions. CORROSION/98, 1998, NACE International, Houston, TX, Paper No. 51.

- [115] Sun W, Nescic S, Woollam RC. The effect of temperature and ionic strength on iron carbonate (FeCO_3) solubility limit. *Corros Sci.* 2009;51(6):1273–1276.
- [116] Ikeda A, Ueda M, Mukai S, et al. CO_2 behavior of carbon and Cr steels. In: Hausler RH, editor. *Advances in CO_2 corrosion*. Houston (TX): NACE; 1984. p. 39.
- [117] Eriksrud E, Sontvedt T. Effect of flow on CO_2 corrosion rates in real and synthetic formation waters. In: Hausler RH, editor. *Advances in CO_2 corrosion*. Houston (TX): NACE; 1984. p. 20.
- [118] Li W, Xiong Y, Brown B, et al. Measurement of wall shear stress in multiphase flow and its effect on protective FeCO_3 corrosion product layer removal. *CORROSION/2015*, Dallas, TX, 2015, NACE International.
- [119] Patchigolla K, Oakey JE, Anthony EJ. Understanding dense phase CO_2 corrosion problems. *Energy Proc.* 2014;63:2493–2499.
- [120] Farelas F, Choi YS, Nescic S. Effects of CO_2 phase change, SO_2 content and flow on the corrosion of CO_2 transmission pipeline steel. *CORROSION/2012*, Salt Lake City, UT, USA, 2012, NACE International, Paper No. C2012-0001322.
- [121] Yevtushenko O, Bäßler R, Carrillo-Salgado I. Corrosion stability of piping steels in a circulating supercritical impure CO_2 environment. *CORROSION/2013*, Orlando, FL, USA, 2013, NACE International, Paper No. 2372.
- [122] Crolet JL, Thevenot N, Dugstad A. Role of free acetic acid on the CO_2 corrosion of steels. *CORROSION/99*, NACE, International, Houston, TX, USA, Paper No. 24, 1999.
- [123] Hemmingsen T, Vangdal H, Valand T. Formation of ferrous sulfide film from sulfite on steel under anaerobic conditions. *Corrosion.* 1992;48(6):475–481.
- [124] Alowitz MJ, Scherer MM. Kinetics of nitrate, nitrite, and Cr(VI) reduction by iron metal. *Environ Sci Technol.* 2002;36:299–306.
- [125] Das GK, Anand S, Acharya S, et al. Preparation and decomposition of ammoniojarosite at elevated temperatures in $\text{H}_2\text{O}-(\text{NH}_4)_2\text{SO}_4\text{-H}_2\text{SO}_4$ media. *Hydrometallurgy.* 1995;38(3):263–276.
- [126] Vitse F, Nescic S, Gunaltun Y, et al. Mechanistic model for the prediction of top-of-the-line corrosion risk. *Corrosion.* 2003;59(12):1075–1084.
- [127] Russick EM, Poulter GA, Adkins CLJ, et al. Corrosive effects of supercritical carbon dioxide and cosolvents on metals. *J Supercrit Fluids.* 1996;9(1):43–50.
- [128] Corvo F, Reyes J, Pérez T, et al. Role of NO_x in materials corrosion and degradation. *Rev Cenic Ciencias Químicas.* 2010;41:1–10.
- [129] Fang H, Young D, Nešić S. Elemental sulfur corrosion of mild steel at high concentrations of sodium chloride. *CORROSION/2009*, Atlanta, GA, USA, Paper No. 2592, 2009, NACE International.
- [130] Boden PJ, Maldonado-Zagal SB. Hydrolysis of elemental sulfur in water and its effects on the corrosion of mild steel. *Br Corros J.* 1982;17:116–120.
- [131] White V, Torrente-Murciano L, Sturgeon D, et al. Purification of oxyfuel-derived CO_2 . *Energy Proc.* 2009;1(1):399–406.
- [132] Allam IM, Arlow JS, Saricimen H. Initial stages of atmospheric corrosion of steel in the Arabian Gulf. *Corros Sci.* 1991;32(4):417–432.
- [133] Bockris JO, Drazic D, Despic A. The electrode kinetics of the deposition and dissolution of iron. *Electrochim Acta.* 1961;4:325–361.
- [134] Ma H, Cheng X, Li G, et al. The influence of hydrogen sulfide on corrosion of iron under different conditions. *Corros Sci.* 2000;42(10):1669–1683.
- [135] Zheng Y, Ning J, Brown B, et al. Investigation of electrochemical reaction kinetic of direct H_2S reduction using 316L RCE. *CORROSION/2015*. Vancouver, 2015, NACE International, Paper No. 7340.
- [136] Zhang GA, Liu D, Guo XP. Corrosion behaviour of N80 carbon steel in formation water under dynamic supercritical CO_2 condition. *Corros Sci.* 2017. DOI:10.1016/j.corsci.2017.02.012.
- [137] Kahyarian A, Singer M, Nescic S. Modeling of uniform CO_2 corrosion of mild steel in gas transportation systems: a review. *J Nat Gas Sci Eng.* 2016;29:530–549.
- [138] de Waard C, Milliams DE. Prediction of carbonic acid corrosion in natural gas pipelines. *First International Conference on the Internal and External Corrosion of Pipes*, University of Durham, UK; 1975.
- [139] Anon. 'NORSOK standard M-506. CO_2 corrosion rate calculation model', in 'Rev. 2', March 2005.
- [140] Gunaltun YM. Combining research and field data for corrosion rate prediction. *CORROSION/1996*, 1996, NACE International, Houston, TX, Paper No. 96027.
- [141] Nescic S, Nordsveen M, Nyborg R, et al. A mechanistic model for CO_2 corrosion with protective iron carbonate films. *CORROSION/2001*, 2001, NACE International, Houston, TX, Paper No. 01040.
- [142] Dayalan E, Moraes FDD, Shirazi SA, et al. CO_2 corrosion prediction in pipe flow under FeCO_3 scale-forming conditions. *CORROSION/1998*, 1998, NACE International, Houston, TX, Paper No. 98051.
- [143] Nescic S, Cai J, Lee K-L. A multiphase flow and internal corrosion prediction model for mild steel pipelines. *CORROSION/2005*, 2005, NACE International, Houston, TX, Paper No. 05556.
- [144] Nescic S, Li H, Sormaz D, et al. A free open source mechanistic model for prediction of mild steel corrosion. 17th International Corrosion Congress, Las Vegas, NV, USA, 2008, NACE International, Paper No. 2659.
- [145] ICMT. Multicorp 5.2 Help: <http://www.icmt.ohio.edu/software/multicorp/multicorp%205/help/Multicorp%205%20Help.pdf>, 2017 [cited 2017 Feb 25].
- [146] Zheng Y, Ning J, Brown B, et al. Electrochemical model of mild steel corrosion in a mixed $\text{H}_2\text{S}/\text{CO}_2$ aqueous environment in the absence of protective corrosion product layers. *Corrosion.* 2015;71(3):316–325.
- [147] Zheng Y, Ning J, Brown B, et al. Advancement in predictive modeling of mild steel corrosion in CO_2 and H_2S containing environments. *Corrosion.* 2016;72(5):679–691.
- [148] Zheng Y, Ning J, Brown B, et al. Electrochemical model of mild steel corrosion in mixed $\text{H}_2\text{S}/\text{CO}_2$ environment. *CORROSION/2015*, San Antonio, TX, 2014, NACE International, Paper No. 3907.
- [149] Seiersten M, Kongshaug KO. Materials selection for capture, compression, transport and injection of CO_2 . In: Thomas DC, editor. *Carbon dioxide capture for storage in deep geologic formations*. Amsterdam: Elsevier Science; 2005. p. 937–953.
- [150] Nordsveen M, Nescic S, Nyborg R, et al. A mechanistic model for carbon dioxide corrosion of mild steel in the presence of protective iron carbonate films – part 1: theory and verification. *Corrosion.* 2003;59(5):443–456.
- [151] Nescic S, Lee KLJ. A mechanistic model for carbon dioxide corrosion of mild steel in the presence of protective iron carbonate films – part 3: film growth model. *Corrosion.* 2003;59(7):616–628.
- [152] Nescic S, Nordsveen M, Nyborg R, et al. A mechanistic model for carbon dioxide corrosion of mild steel in the presence of protective iron carbonate films – part 2: a numerical experiment. *Corrosion.* 2003;59(6):489–497.
- [153] Nescic S, Postlethwaite J, Olsen S. An electrochemical model for prediction of corrosion of mild steel in aqueous carbon dioxide solutions. *Corrosion.* 1996;52(4):280–294.
- [154] Nescic S, Wang S, Cai J, et al. Integrated CO_2 corrosion – multiphase flow model. *SPE International Symposium on Oilfield Corrosion*, Aberdeen, UK, 2004, Society of Petroleum Engineers.
- [155] Graedel TE. GILDES model studies of aqueous chemistry.1. Formulation and potential applications of the multi-regime model. *Corros Sci.* 1996;38(12):2153–2180.
- [156] Ge X, Wang X, Zhang M, et al. Correlation and prediction of activity and osmotic coefficients of aqueous electrolytes at 298.15 K by the modified TCPC model. *J Chem Eng Data.* 2007;52(2):538–547.
- [157] Mullin JW. *Crystallisation*. London: Butterworths; 1972.
- [158] Revie RW. *Uhlig's corrosion handbook*. New York (NY): Wiley; 2000.
- [159] Paul S, Shepherd R, Bahrami A, et al. Material selection for supercritical CO_2 transport. *The First International Forum on the transportation of CO_2 by Pipeline*, 2010, Gateshead, UK.
- [160] Paul S, Shepherd R, Woollin W. Material selection for supercritical CO_2 transport. *The Second International Forum on the Transportation of CO_2 by Pipelines*, Newcastle, UK, 22–23 June 2011.

- [161] Paul S, Shepherd R, Woollin P. Selection of materials for high pressure CO₂ transport. The Third International Forum on the Transportation of CO₂ by Pipeline, Newcastle, UK, June 2012.
- [162] Cheng Y, Li Z, Bi H, et al. Research on the CO₂ corrosion inhibitor technology in oil and gas fields. In: Wu J, Lu X, Xu H, et al. editor. Resources and sustainable development, Pts 1–4; 2013. p. 1240–1245.
- [163] Elena Olvera-Martinez M, Mendoza-Flores J, Genesca J. CO₂ corrosion control in steel pipelines. Influence of turbulent flow on the performance of corrosion inhibitors. *J Loss Prev Process Ind.* 2015;35:19–28.
- [164] Jaal RA, Ismail MC, Ariwahjoedi B. A review of CO₂ corrosion inhibition by imidazoline-based inhibitor. *Icper 2014 – 4th International Conference on Production, Energy and Reliability*, 2014.
- [165] Olivares GZ, Gayosso MJH, Mendoza JLM. Corrosion inhibitors performance for mild steel in CO₂ containing solutions. *Mater Corros.* 2007;58(6):427–437.
- [166] Liu H, Gu T, Zhang G, et al. Corrosion inhibition of carbon steel in CO₂-containing oilfield produced water in the presence of iron-oxidizing bacteria and inhibitors. *Corros Sci.* 2016;105:149–160.
- [167] Zhang C, Duan H, Zhao J. Synergistic inhibition effect of imidazoline derivative and l-cysteine on carbon steel corrosion in a CO₂-saturated brine solution. *Corros Sci.* 2016;112:160–169.
- [168] Zhao J, Duan H, Jiang R. Synergistic corrosion inhibition effect of quinoline quaternary ammonium salt and Gemini surfactant in H₂S and CO₂ saturated brine solution. *Corros Sci.* 2015;91:108–119.
- [169] Gulbrandsen E, Nesic S, Stangeland A, et al. Effect of precorrosion on the performance of inhibitors for CO₂ corrosion of carbon steel. *CORROSION/98*, San Diego, CA, USA, 1998/1/1/, 1998, NACE International, Paper No. 13.
- [170] Nam ND, Mathesh M, Hinton B, et al. Rare earth 4-hydroxycinnamate compounds as carbon dioxide corrosion inhibitors for steel in sodium chloride solution. *J Electrochem Soc.* 2014;161(12):C527–C534.
- [171] Nam ND, Somers A, Mathesh M, et al. The behaviour of praseodymium 4-hydroxycinnamate as an inhibitor for carbon dioxide corrosion and oxygen corrosion of steel in NaCl solutions. *Corros Sci.* 2014;80:128–138.
- [172] Choi Y-S, Nešić S. Corrosion behavior of carbon steel in supercritical CO₂-water environments. *CORROSION/2009*, Atlanta, GA, USA, 2009, NACE International, Paper No. 09256.
- [173] Choi Y-S, Nešić S. Effect of impurities on the corrosion behavior of carbon steel in supercritical CO₂-water environments. *CORROSION/2010*, San Antonio, TX, USA, 2010, NACE International, Paper No. 10196.
- [174] Choi Y-S. Effect of water content on the corrosion behavior of carbon steel in supercritical CO₂ phase with impurities. *CORROSION/2011*, Houston, TX, USA, 2011, NACE International, Paper No. 11377.
- [175] Ruhl AS, Kranzmann A. Investigation of pipeline corrosion in pressurized CO₂ containing impurities. *Energy Proc.* 2013;37:3131–3136.
- [176] Hua Y, Barker R, Neville A. Understanding the influence of SO₂ and O₂ on the corrosion of carbon steel in water-saturated supercritical CO₂. *CORROSION/2015*, Dallas, TX, USA, 2015, NACE International, Paper No. 5832.

Appendix A

Table A1. Summary of the test conditions for steel corrosion in dense CO₂ with impurities

Year	Researchers	Materials	Temperature (K)	Pressure (MPa)	Time (h)	Impurities	Flow (rev min ⁻¹)	General corrosion rate (mm/y)
1975	Schremp and Roberson [10]	X60, AISI 4140	276, 295	13.8	1008	H ₂ O: 800–1000 ppm H ₂ S: 600–800 ppm	Loop	Less than 5.08×10^{-4}
1996	Russick et al. [127]	304 LSS, 306 SS, C1018	323	24.138	24	H ₂ O	Static	Weight change: -1.06 to $+0.77 \mu\text{g cm}^{-2}$ 2.54×10^{-3} to 1.016×10^{-2} 1.27×10^{-3} 2.54×10^{-5} 5.08×10^{-4}
1996	Propp et al. [12]	Iron	Up to: 456	8.7–12.3	4964	Pure CO ₂	Loop	
		304 SS, 316 SS	Up to: 511	9.8–15.7	742–9177	Pure CO ₂		
		304 SS	538	9.3–16.5	2300	Methanol: 10 wt-%		
		304 SS	473	13.8–16.5	3900	H ₂ O: 1 wt-%		
2009	Thodla et al. [80]	CS	304	7.9	3.5	H ₂ O: 100, 1000 ppm MEA: 100, 1000 ppm	Static	About 0.01–2
2009	Choi and Nestic [25, 172]	X65	323	4.0–8.0	24	H ₂ O: saturated	Static	About 0.2–0.4
2009	McGrail et al. [35]	ANSI 01 carbon steel	295	6.25	1008	H ₂ O: 610 ppmw	Static	Not given
		ANSI 01 carbon steel	295	6.32	504	H ₂ O: 998 ppmw		
		X70	297	8.2	1176	H ₂ S: 321 ppmw H ₂ O: 408 ppmw		
2010	Choi and Nešić [23,173]	X65, 13Cr	323	8.0	24–120	H ₂ O: saturated SO ₂ : 1 vol.-% O ₂ : ~5.1 bar	Static	Up to 7
2010	Ayello et al. [104]	CS 1010	318	7.58, 13.1	5	H ₂ O: 100–2000 ppm O ₂ : 100 ppm SO ₂ : 100 ppm NO ₂ : 100 ppm	Static	12
2011	Dugstad et al. [27]	X65	283–323	10.0	72–720	SO ₂ , O ₂ , H ₂ O	0–3 m s ⁻¹	About 0.01–40
2011	Choi [174]	X65	323	8.0	24, 120	H ₂ O: 650–3000 ppmv O ₂ : ~3.3 bar SO ₂ : 1 vol.-% H ₂ SO ₃ : 650 ppmv	Static	3.7
2011	Dugstad et al. [63]	X65	298	10	3–20 days	H ₂ O: 488–1222 ppmv SO ₂ : 100–344 ppmv NO ₂ : 96–478	Rotating autoclave: 3 rev min ⁻¹	Up to 1.6
2011	Xiang et al. [45]	X70, Iron	323	10	288	H ₂ O: saturated SO ₂ : 0.2–2.0 vol.-% O ₂ : 1000 ppmv	120	0.19–0.88, 0.34–1.35
2011	Zhang et al. [48]	38Mn6/C75 X65 X20Cr13 X2CrNiMoN22-5-3 X1NiCrMoCu 25-20-5	323–403	9.5–21.5	96	H ₂ O: 1.5–1000 g	4 m s ⁻¹	~0.8
2012	Paschke and Kather [90]	X12Cr13 X5CrNiCuNb16-4 L360NB L485MB	333, 423	11	168	H ₂ O: 0–1000 ppmv O ₂ : 4.7 vol.-%, 0.67 vol.-%, 100 ppmv NO: 100 ppmv SO ₂ : 70 ppmv CO: 50 ppmv Ar + N ₂ : 10.37 vol.-%, 1.3 vol.-%, 200 ppmv	Static	<0.1
2012	Ruhl and Kranzmann [37]	X42	333	10	120	H ₂ O: 0.5–1 mL HNO ₃ (65 wt-%): 0.2–1 mL H ₂ SO ₄ (96 wt-%): 0.2–1 mL HCl (37 wt-%): 1 mL	Static	Weight loss < 500 mg
2012	Xiang et al. [46]	X70	323	10	120		120	0.005–1.46

(Continued)

Table A1. Continued.

Year	Researchers	Materials	Temperature (K)	Pressure (MPa)	Time (h)	Impurities	Flow (rev min ⁻¹)	General corrosion rate (mm/y)
2013	Collier et al. [26]	304L, 316L, X42, X60	307–322	9.48–10.3	110–120	H ₂ O: 0.17–3.0 g SO ₂ : 2 vol.-% O ₂ : 1000 ppmv	100	<4 mpy
2013	Farelas et al. [88,120]	X65	298, 323	8	24	H ₂ O: 10–100 g O ₂ : 3 vol.-%	1000	Up to 3.48
2013	Ruhl and Kranzmann [175]	X42	333	10	Up to 240	Nitric acid (65 wt-%): 22.7 μL	Static	Weight increase < 5 mg
2013	Sim et al. [40]	CS	323	7.6	168	H ₂ O: 10 g L ⁻¹ NaCl: 1 g L ⁻¹ Na ₂ SO ₄ : 1–3 g L ⁻¹ NaNO ₃ : 1–3 g L ⁻¹ HNO ₃ : 10 g L ⁻¹ pH 4	Static	Mass loss: 1.63–2.40 mg
2013	Xiang et al. [43]	X70	298–366	10	120	H ₂ O: 5.0 g SO ₂ : 2 vol.-% O ₂ : 0.02 mol	120	1.10–3.06
2013	Xiang et al. [15]	X70	323	10	24–192	H ₂ O: 3.0 g SO ₂ : 2 vol.-% O ₂ : 1100 ppmv	120	0.73–1.95
2013	Xiang et al. [44]	X70, Iron	323	12	454	H ₂ O: 15 g SO ₂ : 2.5 vol.-% O ₂ : 700 ppmv	120	1.16, 0.59
2013	Yevtushenko et al. [121]	Alloy 31 L360 NB Iron X20Cr13 X46Cr13 X2CrMnNiN22-5-2	333	10	168	H ₂ O: 1000 ppmv SO ₂ : 70 ppmv NO ₂ : 100 ppmv CO: 750 ppmv O ₂ : 8100 ppmv	Loop	Up to 0.03
2014	Hua et al. [28]	X65	308, 323	8	14–48	H ₂ O: 300–34 000 ppm	Static	Up to 0.1
2014	Sim et al. [39]	CS	313	8	168	H ₂ O: 100–50 000 ppmv	Static	Mass loss: 2.07–5.47 mg
2014	Yevtushenko and Bäßler [79]	X52 UNS S42000 UNS G41400	333	10	7, 30, and 186 days	H ₂ O: 500–1000 ppmv SO ₂ : 70 ppmv NO ₂ : 100 ppmv CO: 750 ppmv O ₂ : 8100 ppmv	Loop	Up to 0.025 mm/y
2014	Brown et al. [62]	X65	277, 323	10	168	H ₂ O: 50, 500 ppmv	Rotating autoclave: 3 rpm	Up to 0.275
2014	Dugstad et al. [64]	X65	273–323	10	74–147	H ₂ O: 300 ppmv O ₂ : 350 ppmv SO ₂ : 100 ppmv NO ₂ : 100 ppmv H ₂ S: 100 ppmv	Rotating autoclave: 3 rev min ⁻¹	<0.1
2014	Patchigolla et al. [119]	X60 X70 X100	308	9.5	50–1100	H ₂ O: 3300 ppm SO ₂ : 500 ppm	50 g min ⁻¹	Metal loss: 1.00705–6.84080 μm
2015	Zeng et al. [103]	X42, X60, X80, and X100	308, 318	5.86–10.34	120	H ₂ O: saturated O ₂ : 0.14, 0.28 MPa	0–500	0–0.163
2015	Jiang et al. [34]	X65	298, 308	8	3, 14 days	H ₂ O: 600 ppm~saturated	Static	<10
2015	Choi et al. [24]	CS, 1Cr, 3Cr	298, 353	8–12	24, 48	H ₂ O: saturated, 100 ppmv H ₂ S: 200 ppmv	Static	~0.44
2015	Hua et al. [29]	X65	323	8	14–48	H ₂ O: saturated	Static	<0.1
2015	Hua et al. [13]	X65	308	8	14–168	H ₂ O: 34000 ppm	Static	~0.1
2015	Hua et al. [32,176]	X65	308	8	48		Static	<1

2015	Hua et al. [30]	X65	308	8	48	H ₂ O: saturated SO ₂ : 0–100 ppm mol O ₂ : 0, 20 ppm mol H ₂ O: 0–34 000 ppm SO ₂ : 0–100 ppm O ₂ : 0, 20 ppm	Static	<1
2015	Hua et al. [31]	X65	308	8	48	H ₂ O: 300–34 000 ppm O ₂ : 0–1000 ppm	Static	<0.13
2016	Sun et al. [41]	X65	323	10	240	H ₂ O: 10 g O ₂ : 2000 ppmv H ₂ S: 2000 ppmv	Static	<0.35
2016	Sun et al. [16]	X65	323	10	120	H ₂ O: saturated SO ₂ : 1000 ppmv O ₂ : 1000 ppmv H ₂ S: 1000 ppmv	Static	0.015–1.439
2016	Sun et al. [91]	X65	323	10	24, 120	O ₂ , SO ₂ , H ₂ S, and NO ₂ : 1000 ppmv	Static	~1.9
2016	Wei et al. [102]	P110, 3Cr, 316L	353	10	240	H ₂ O: saturated	1 m s ⁻¹	0–10
2016	Wei et al. [42]	X65	353	10	240	H ₂ O: saturated H ₂ S: 0, 50 ppm	1 m s ⁻¹	0.17, 0.24
2016	Xu et al. [47]	X70	323	10	72	H ₂ O: RH 45–100% SO ₂ : 2.0 vol.-% O ₂ : 1.0 vol.-%	120	0.03–1.78
2016	Xu et al. [113]	X60, X65, X70, X80	323	8–12	72	H ₂ O: 1600–3000 ppmv SO ₂ : 3000 ppmv O ₂ : 1000 ppmv	120	0.01–0.94
2017	Xu et al. [105]	X70	323	10	72	H ₂ O: RH 45–100% SO ₂ : 2.0 vol.-% O ₂ : 0.1–2.0 vol.-%	120	0.03–1.61
2017	Tang et al. [86]	X65	323	8	96	H ₂ O: 100 mL O ₂ : 0–475 mg L ⁻¹	Static	0.25–1.52